

Mycobacterial helicase Lhr abets resistance to DNA crosslinking agents mitomycin C and cisplatin

Garrett M. Warren¹, Anam Ejaz¹, Allison Fay², Michael S. Glickman² and Stewart Shuman^{1,*}

¹Molecular Biology Program, Memorial Sloan Kettering Cancer Center, NY, NY 10065, USA and ²Immunology Program, Memorial Sloan Kettering Cancer Center, NY, NY 10065, USA

Received July 24, 2022; Revised December 05, 2022; Editorial Decision December 06, 2022; Accepted December 12, 2022

ABSTRACT

Mycobacterium smegmatis Lhr exemplifies a novel clade of helicases composed of an N-terminal ATPase/helicase domain (Lhr-Core) and a large C-terminal domain (Lhr-CTD) that nucleates a unique homo-tetrameric quaternary structure. Expression of Lhr, and its operonic neighbor *Nei2*, is induced in mycobacteria exposed to mitomycin C (MMC). Here we report that *lhr* deletion sensitizes *M. smegmatis* to killing by DNA crosslinkers MMC and cisplatin but not to killing by monoadduct-forming alkylating agent methyl methanesulfonate or UV irradiation. Testing complementation of MMC and cisplatin sensitivity by expression of Lhr mutants in Δlhr cells established that: (i) Lhr-CTD is essential for DNA repair activity, such that Lhr-Core does not suffice; (ii) ATPase-defective mutant D170A/E171A fails to complement; (iii) ATPase-active, helicase-defective mutant W597A fails to complement and (iv) alanine mutations at the CTD-CTD interface that interdict homo-tetramer formation result in failure to complement. Our results instate Lhr's ATP-driven motor as an agent of inter-strand crosslink repair *in vivo*, contingent on Lhr's tetrameric quaternary structure. We characterize *M. smegmatis* *Nei2* as a monomeric enzyme with AP β -lyase activity on single-stranded DNA. Counter to previous reports, we find *Nei2* is inactive as a lyase at a THF abasic site and has feeble uracil glycosylase activity.

INTRODUCTION

Helicases have wide-ranging functions in DNA repair, whereby they couple the chemical energy of NTP hydrolysis to mechanical changes in nucleic acid secondary structures or to structural remodeling of protein-nucleic acid assemblies. Helicase variations in directionality of translocation, nucleic acid recognition, auxiliary domains, quater-

nary structure, and protein-protein interactions facilitate their specialization for particular DNA repair pathways or types of DNA damage.

The *Mycobacterium smegmatis* helicase Lhr is the founder of a new clade of superfamily 2 (SF2) DNA helicase, by virtue of its signature domain structure and its distinctive DNA interface (1–3). Lhr is a 1507-amino acid (aa) nucleic acid-dependent ATPase/dATPase that uses ATP hydrolysis to drive unidirectional 3' to 5' translocation along single-strand (ss) DNA (the tracking strand) and to unwind duplexes *en route* (1). The strand displaced by the translocating Lhr helicase can be either RNA or DNA, with the former being preferred (1). The ATPase, DNA translocase, and RNA:DNA helicase activities of mycobacterial Lhr are encompassed within the N-terminal 856-aa segment (1). This autonomous helicase, referred to as Lhr-Core, consists of two N-terminal RecA-like modules (aa 8–230 and 231–435, respectively), a winged helix (WH) domain (aa 436–529), and a unique core C-domain (aa 530–856) that adopts a novel fold (2) (Figure 1A,B). All four protein domains of Lhr-Core contribute to an extensive interface with the DNA tracking strand (Figure 1B). Lhr Core is a monomer in solution and *in crystallo* (2,3).

The large C-terminal domain (CTD) of mycobacterial Lhr, though not required for Lhr's motor activity, serves to nucleate a homo-tetrameric quaternary structure of full-length Lhr (3). The isolated Lhr-CTD is itself a homo-tetramer. The cryo-EM structure of Lhr-CTD (3) revealed an assembly of four CTD protomers (labeled CTD-I, -II, -III, and IV in Figure 1C) that interact to form a cylindrical structure 87 Å in diameter and 110 Å long (Figure 1C). CTD-I and CTD-II are in a tail-to-tail arrangement with CTD-III and CTD-IV, with 2-fold symmetry about the y-axis in the view shown in Figure 1C. The CTD protomer is composed of a series of five winged-helix (WH) modules (named WH2–6 in series with WH1 in the Core domain) and a β -barrel module (Figure 1A).

An Lhr-CTD subdomain, comprising three tandem WH modules and the β -barrel, is structurally homologous to AlkZ, a bacterial DNA glycosylase that recognizes and excises inter-strand DNA crosslinks (4,5). This

*To whom correspondence should be addressed. Tel: +1 212 639 7145; E-mail: s-shuman@ski.mskcc.org

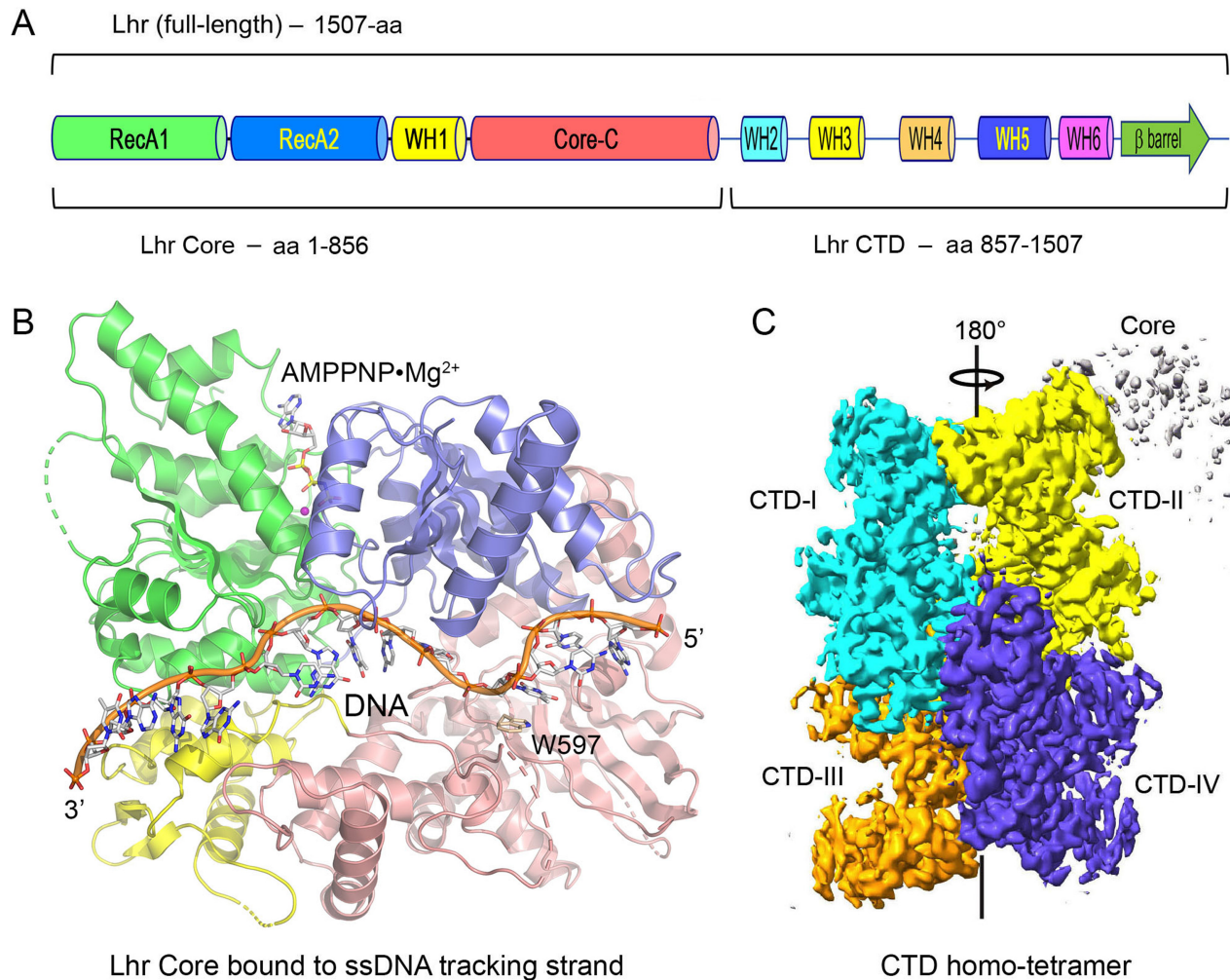


Figure 1. Lhr domain organization and structure. (A) Lhr-FL (aa 1–1507) is composed of a Core helicase domain (aa 1–856) and a CTD tetramerization domain (aa 857–1507). Lhr-Core consists of two N-terminal RecA-like modules (green and blue, respectively), a winged helix (WH) module (yellow), and a unique core C-domain module (red). Lhr-CTD consists of five winged-helix (WH) modules and a β -barrel module. (B) The crystal structure of Lhr-Core in complex with AMPPNP·Mg²⁺ and ssDNA shows that all four protein domains of Lhr-Core contribute to an extensive interface with the DNA tracking strand. The Trp597 side chain (stick model with beige carbons) that stacks on a tracking strand nucleobase is essential for helicase activity but not for ssDNA-dependent ATPase activity. (C) The cryo-EM structure of the Lhr-CTD homo-tetramer, depicted as a surface model colored by protomer: CTD-I (cyan), and CTD-II (yellow), CTD-III (gold) and CTD-IV (blue); and with 2-fold symmetry about the y-axis.

homology is noteworthy given that mycobacterial Lhr, along with its operonic neighbor Nei2 (a putative DNA glycosylase/lyase), is transcriptionally upregulated by the LexA/RecA-independent PafBC pathway in response to DNA damage by the inter-strand crosslinker mitomycin C (MMC) (6–9). Lhr/Nei2 expression is also induced by UV irradiation and by treatment with ciprofloxacin (a type II topoisomerase poison) and nargenicin (an inhibitor of replication polymerase DnaE1) (10,11).

Genome-wide transposon mutagenesis and CRISPR knockdown studies in *M. tuberculosis* and *M. smegmatis* have indicated that Δ lhr and Δ nei2 gene disruption mutants, or lhr and nei2 gene-silenced strains, retained viability under laboratory growth conditions (12,13). Our first aim in the present study was to interrogate the role of Lhr in mycobacterial DNA repair. To that end, we constructed a Δ lhr strain in which the coding sequence was deleted. We report that loss of Lhr sensitizes *M. smegmatis* to killing by DNA crosslinkers MMC and cisplatin but does not sensitize to

killing by the monoadduct-forming alkylating agent methyl methanesulfonate (MMS) or by UV irradiation. Testing for complementation of MMC and cisplatin sensitivity by expression of Lhr mutants in Δ lhr cells showed that Lhr's ATPase motor and its homo-tetrameric quaternary structure are essential for Lhr function in crosslink repair *in vivo*. Our second aim was to biochemically characterize Nei2 as an initial step toward establishing its potential DNA repair functions. We find that Nei2 is a monomeric protein with brisk AP lyase activity that proceeds via a borohydride-trappable Schiff base intermediate. We discuss potential scenarios whereby Lhr and Nei2 might collaborate in the repair of DNA crosslinks.

MATERIALS AND METHODS

Deletion of lhr in *M. smegmatis*

In-frame deletion of the entire open reading frame (ORF) of lhr (spanning aa 1–1507) in wild-type *M. smegmatis*

was achieved by a two-step allelic exchange process as described previously (14). In this way, we minimized a potential polar effect on expression of the 3'-flanking *nei2* gene (Figure 2A). Briefly, a 5'-flanking genomic fragment consisting of the 650-bp upstream of the annotated *lhr* start codon was PCR-amplified from *M. smegmatis* mc²155 genomic DNA with primers AF882 (5'-GTCGCCTTCGGGCATGCCTAGCCATGGTGCAC) and AF883 (5'-CGCCTGACGCCCATTTATCGCGGCCACAGCG). A 3'-flanking genomic fragment starting from the *lhr* stop codon and spanning 685-bp of downstream DNA was PCR-amplified with primers AF880 (5'-CCGCCCTAGGCAATTGCATACACCCACAGCTGG) and AF881 (5'-GGTGCACCATGGCTAGGCATGCCGAAGGCGAC). The *lhr* flanks were inserted adjacent to each other in linearized pAJF067, a mycobacterial suicide plasmid bearing a hygromycin-resistance marker and counterselectable markers *sacB* and *galK*. The resulting plasmid pAJF568 was then transformed into *M. smegmatis* mc²155. Hygromycin-resistant Δlhr *lhr*⁺ merodiploid strains were genotyped to verify targeted insertion and then subjected to sucrose and 2-deoxy-galactose counterselection for loss of the intervening *sacB* and *galK* markers. PCR amplification of the genomic *lhr* locus with primers AF884 (5'-CATCCGAACGAGTACCAG) and AF889 (5'-GGCACACGGGGCACCAATAG) and sequencing of the PCR product were performed to confirm the final unmarked Δlhr mutant strain. The same methods were applied to delete the entire *lhr* ORF in an *M. smegmatis* $\Delta uvrD1$ strain (15) to yield a Δlhr $\Delta uvrD1$ double-mutant.

Complementation of Δlhr by expression of wild-type Lhr and Lhr mutants

DNA fragments encoding full-length Lhr or Lhr-Core (aa 1–856) were PCR-amplified from *M. smegmatis* genomic DNA with primers that introduced a NotI site 225 bp upstream of the start codon (thereby including the putative native *lhr* promoter) and a HindIII site downstream of the native or newly installed stop codon. The PCR products were digested with NotI and HindIII and ligated into the episomal kanamycin-resistance plasmid pMV261 that had been digested with NotI and HindIII to yield pLhr-FL/WT and pLhr-Core. Alanine mutations D170A/E170A (ATPase-defective) and W597A (ATPase-active; helicase-defective) were introduced by PCR amplification with mutagenic primers. The D170A/E170A or W597A mutant PCR products were digested and ligated into pLhr-FL in lieu of the fragment between NotI and SphI sites or SphI and EcoRI sites, respectively. Alanine substitution mutations H1199A-R1206A-R1286A at the CTD tetramer interface were introduced by PCR amplification of a synthetic gene construct (purchased from Azenta Life Sciences) containing the three alanine substitutions and codon-optimized for *Escherichia coli* expression. The H1199A-R1206A-R1286A PCR product was digested and ligated into pLhr-FL/WT in lieu of a fragment between EcoRI and HindIII sites. All plasmid inserts were sequenced to verify that no unintended coding changes were acquired during amplification and cloning. Wild-type and mutant pLhr plasmids were transformed into the *M. smegmatis* Δlhr strain. Control wild-type and

Δlhr strains were transformed with the empty pMV261 vector.

Sensitivity to mitomycin C

Log phase cultures (1.5 ml at A_{600} of 0.3–0.4) of *M. smegmatis* strains grown in Middlebrook 7H9 medium were supplemented with mitomycin C (from Sigma; prepared as a 0.8 mg/ml stock solution in DMSO) at the concentrations specified in figure legends. After incubation for 2 h at 37°C with constant shaking (200 rpm), the control and MMC-treated cells were harvested by centrifugation, washed twice with drug-free 7H9 medium, and resuspended in 7H9 medium to attain equal optical density. Aliquots (2.5 μ l) of serial 10-fold dilutions were spotted on 7H10 agar plates supplemented with 0.5% glycerol, 0.5% dextrose and incubated at 37°C for 3 days. MMC sensitivity experiments were performed with two or three independent biological replicates; representative experiments are shown in Figures 2, 4, 5 and 8.

Sensitivity to cisplatin

Log phase cultures (1.5 ml at A_{600} of 0.3–0.4) of *M. smegmatis* strains grown in 7H9 medium were supplemented with cisplatin (from US Pharmacopeia, prepared as a 2 mg/ml stock solution in 150 mM NaCl) at the concentrations specified in figure legends. After incubation for 1 h at 37°C with constant shaking (200 rpm), the control and cisplatin-treated cells were harvested by centrifugation, washed once with drug-free 7H9 medium, and resuspended in 7H9 medium to attain equal optical density. Aliquots (2.5 μ l) of serial 10-fold dilutions were spotted on 7H10 agar plates supplemented with 0.5% glycerol, 0.5% dextrose and incubated at 37°C for 3 days. Cisplatin sensitivity experiments were performed with two or three independent biological replicates; representative experiments are shown in Figures 2, 4, 5 and 8.

Sensitivity to UV irradiation

M. smegmatis strains were grown to log phase (A_{600} 0.3–0.4) and serial 10-fold dilutions prepared in 7H9 media were spotted on 7H10 agar plates supplemented with 0.5% glycerol, 0.5% dextrose. UV irradiation at the doses specified in the figures was performed with a Spectrolinker XL-1500 UV crosslinker (Spectronic Corp.) fitted with 254 nm bulbs. Immediately after exposure, the plates were wrapped in foil (to prevent repair by photolyase) and incubated at 37°C for 3 days. UV sensitivity experiments were performed with two or three independent biological replicates; a representative experiment is shown in Figure 3.

Sensitivity to MMS

Log phase cultures (1.5 ml at A_{600} of 0.3–0.4) of *M. smegmatis* strains grown in 7H9 medium were supplemented with methyl methanesulfonate (from Sigma, stored as a 1.3 g/ml stock solution in 100% DMSO) at the concentrations specified in figure legends. After incubation for 1 h at 37°C with constant shaking (200 rpm), cold sodium thiosulfate

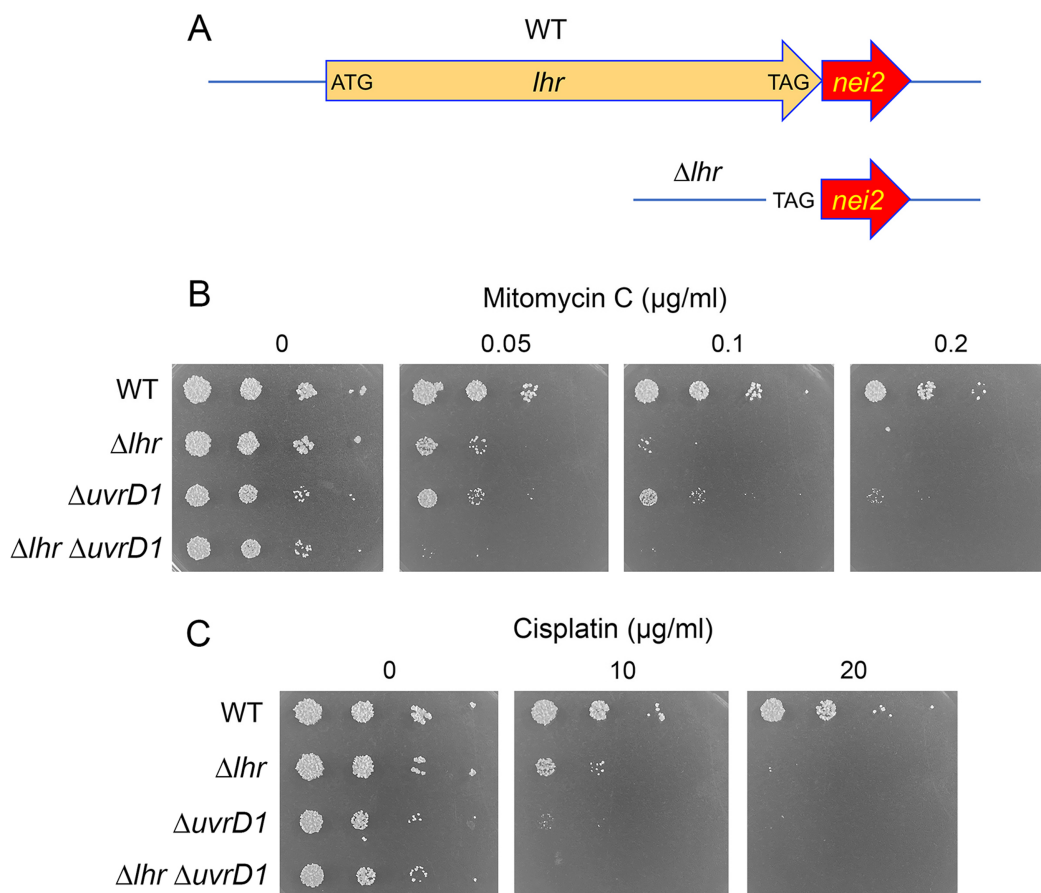


Figure 2. Deletion of *lhr* sensitizes *M. smegmatis* to killing by MMC and cisplatin. (A) Cartoon depiction of the wild-type *M. smegmatis* *lhr-nei2* operon with the respective open reading frames (ORFs) rendered as arrows. ATG and TAG are the start and stop codons that demarcate the *lhr* ORF. The genomic locus of the Δlhr strain is depicted at bottom, wherein the entire *lhr* ORF is deleted and only the *lhr* stop codon remains flanking the unperturbed *nei2* ORF. (B) Wild-type, Δlhr , $\Delta uvrD1$, and $\Delta lhr \Delta uvrD1$ strains were treated with 0, 0.05, 0.1, or 0.2 $\mu\text{g/ml}$ MMC for 2 h at 37°C. (C) Wild-type, Δlhr , $\Delta uvrD1$, and $\Delta lhr \Delta uvrD1$ strains were treated with 0, 10, or 20 $\mu\text{g/ml}$ cisplatin for 1 h at 37°C. Post-treatment, the cells were harvested by centrifugation, washed twice to remove the clastogen, then resuspended and adjusted to equal optical density. Serial tenfold dilutions were spotted on 7H10 agar plates and incubated for 3 days at 37°C to gauge survival.

was added to 5% (v/v) final concentration. The control and MMS-treated cells were harvested by centrifugation, washed once with drug-free 7H9 medium, and resuspended in 7H9 medium to attain equal optical density. Aliquots (2.5 μl) of serial 10-fold dilutions were spotted on 7H10 agar plates supplemented with 0.5% glycerol, 0.5% dextrose and incubated at 37°C for 3 days. MMS sensitivity experiments were performed with two or three independent biological replicates; a representative experiment is shown in Figure 3.

Recombinant Lhr and Lhr mutants

pET28b-based plasmids for bacterial expression of His₁₀Smt3-tagged full-length wild-type Lhr (aa 1–1507), and Lhr-CTD (aa 863–1507) were described previously (3). CTD tetramer interface mutations H1199A-R1206A-R1286A and R915A-T1100A-D1366A were incorporated into synthetic CTD gene fragments purchased from Azena Life Sciences and codon optimized for *E. coli* expression. For expression of the mutated Lhr-CTD proteins, the synthetic DNAs were PCR amplified, digested with

BamHI and NotI, and inserted into pET28b-His₁₀Smt3. For expression of full-length Lhr containing the interface mutants, the PCR products were digested with EcoRI and NotI and inserted into pET28b-His₁₀Smt3-Lhr-FL in lieu of the wild-type EcoRI/NotI fragment. All plasmid inserts were sequenced to verify that no unintended coding changes were acquired during amplification and cloning. Recombinant Lhr, Lhr-CTD, and CTD interface mutants were produced in *E. coli* BL21(DE3) and purified from soluble extracts of 1-liter cultures by serial nickel-affinity, tag removal, HiTrapQ ion exchange chromatography, and Superdex-200 gel filtration steps as described previously (3). Peak fractions were pooled, concentrated by centrifugal ultrafiltration, frozen, and stored at –80°C. Protein concentrations were determined with the BioRad dye reagent using BSA as the standard.

Anti-Lhr antibody

Recombinant full-length tag-free Lhr was produced in *E. coli* and purified to homogeneity from a soluble bacterial extract by sequential affinity chromatography, tag removal,

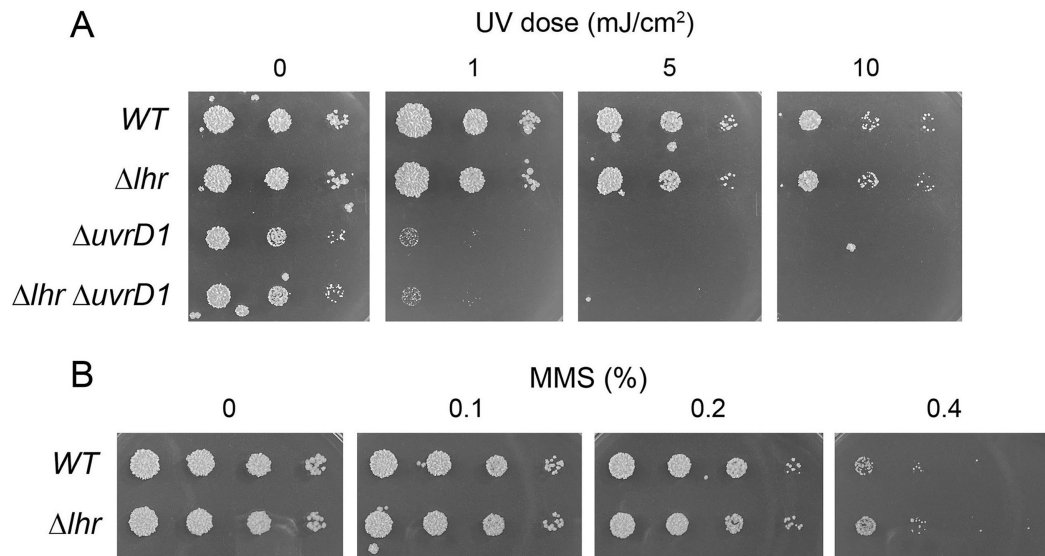


Figure 3. Deletion of *lhr* does not sensitize *M. smegmatis* to killing by UV or MMS. (A) Serial ten-fold dilutions of wild-type, Δlhr , $\Delta uvrD1$, and $\Delta lhr \Delta uvrD1$ cells (adjusted for optical density) were spotted on 7H10 agar plates, which were exposed to the UV doses specified (0, 1, 5, or 10 mJ/cm²). The plates were photographed after incubation in the dark for 3 d at 37°C. (B) Wild-type and Δlhr strains were treated with 0%, 0.1%, 0.2%, or 0.4% MMS for 1 h at 37°C. Post-treatment, sodium thiosulfate was added to 5% final concentration, cells were harvested and washed, and serial ten-fold dilutions of cells were spotted on 7H10 agar plates and incubated for 3 days at 37°C to gauge survival.

anion exchange chromatography, and gel filtration steps as described (3). Rabbit immunization with purified Lhr and preparation of antiserum were performed by Pocono Hills Rabbit Farm and Laboratory (Canadensis, PA) according to their 70 Day Antibody Production Protocol. Anti-Lhr antibody was purified from rabbit serum by affinity chromatography as follows. Purified Lhr (1 mg) was dialyzed against coupling buffer (50 mM HEPES, pH 8.0, 500 mM NaCl, 5% glycerol) and then coupled to 4 ml of Affigel-15 resin (Biorad) during overnight incubation at 4°C. The resin was washed serially with: 100 mM Tris-HCl, pH 7.5; 200 mM glycine, pH 2.6; 1 M Tris-HCl, pH 7.5; and 20 mM Tris-HCl, pH 7.5, 150 mM NaCl. Lhr-coupled resin was then mixed with 8 ml of rabbit immune serum overnight at 4°C on a nutator. The resin was poured into a column and washed thoroughly with 10 mM Tris-HCl, pH 7.5, 150 mM NaCl until no further protein eluted, as gauged by BioRad dye-binding assay of wash fractions. Bound antibodies were eluted with 200 mM glycine, pH 2.6, while collecting fractions (1 ml) in tubes containing 100 μ l of 1 M Tris-HCl, pH 7.5 to adjust the pH. Protein-containing eluate fractions were pooled and dialyzed against buffer containing 200 mM Tris-HCl, pH 7.5, 50 mM NaCl, 0.1 mM EDTA, 0.1 mM β -mercaptoethanol, 5% glycerol.

Western blotting

M. smegmatis cells were harvested from 15 ml log-phase cultures (A_{600} of 0.3 to 0.4) by centrifugation, resuspended in 10 ml of PBS buffer (9.32 mM Na₂PO₄, 0.68 mM NaH₂PO₄, pH 8.0, 150 mM NaCl), re-pelleted by centrifugation and resuspended in 10 ml PBS. After a third centrifugation, the cells were suspended in 200 μ l PBS. Cells were disrupted mechanically with 0.1 mm diameter zirco-

nia beads in a FastPrep-24 instrument (MP Bio) for a total of 3 \times 30 s with 5 min on ice between disruptions. The lysates were mixed with an equal volume of PBS containing 0.25% NP-40 and placed on ice. Aliquots of the samples (40 μ l) were mixed with 10 μ l of SDS loading buffer and then heated at 95°C for 10 min prior to loading onto a 6% polyacrylamide gel containing 0.1% SDS. After SDS-PAGE, the resolved polypeptides were transferred to a PVDF membrane using an iBlot2 apparatus (Invitrogen). The membrane was incubated for 1 h at 22°C with 5% milk in TBST buffer (10 mM Tris-HCl pH 7.5, 150 mM NaCl, 0.1% Tween 20). The membrane was then probed with affinity-purified anti-Lhr diluted 1:1000 in 5% milk/TBST for 16 h at 4°C. The antibody was then removed and the membrane was washed three times with TBST. The membrane was then incubated for 1 h at 22°C with HRP-conjugated anti-Rabbit IgG (produced in donkey, Cytiva) diluted 1:5000 in 5% milk/TBST. After removing the secondary antibody and re-washing the membrane three times with TBST, chemiluminescence was induced by incubating membranes for 1 min with freshly prepared western blot detection reagent (Cytiva). The immunoblots were imaged immediately by using an ImageQuant 800 western blot imaging system (Cytiva).

Recombinant Nei2

The *nei2* ORF (Msmeg_1756) was PCR-amplified from *M. smegmatis* genomic DNA with primers that introduced a NdeI site over the start codon and a XhoI site downstream of the native stop codon. The PCR product was digested with NdeI and XhoI and ligated into pET21b-His6 that had been digested with NdeI and XhoI. The resulting pET21b-Nei2-His6 plasmid encodes full-length Nei2 fused to a C-terminal His6 tag. The plasmid insert was sequenced to

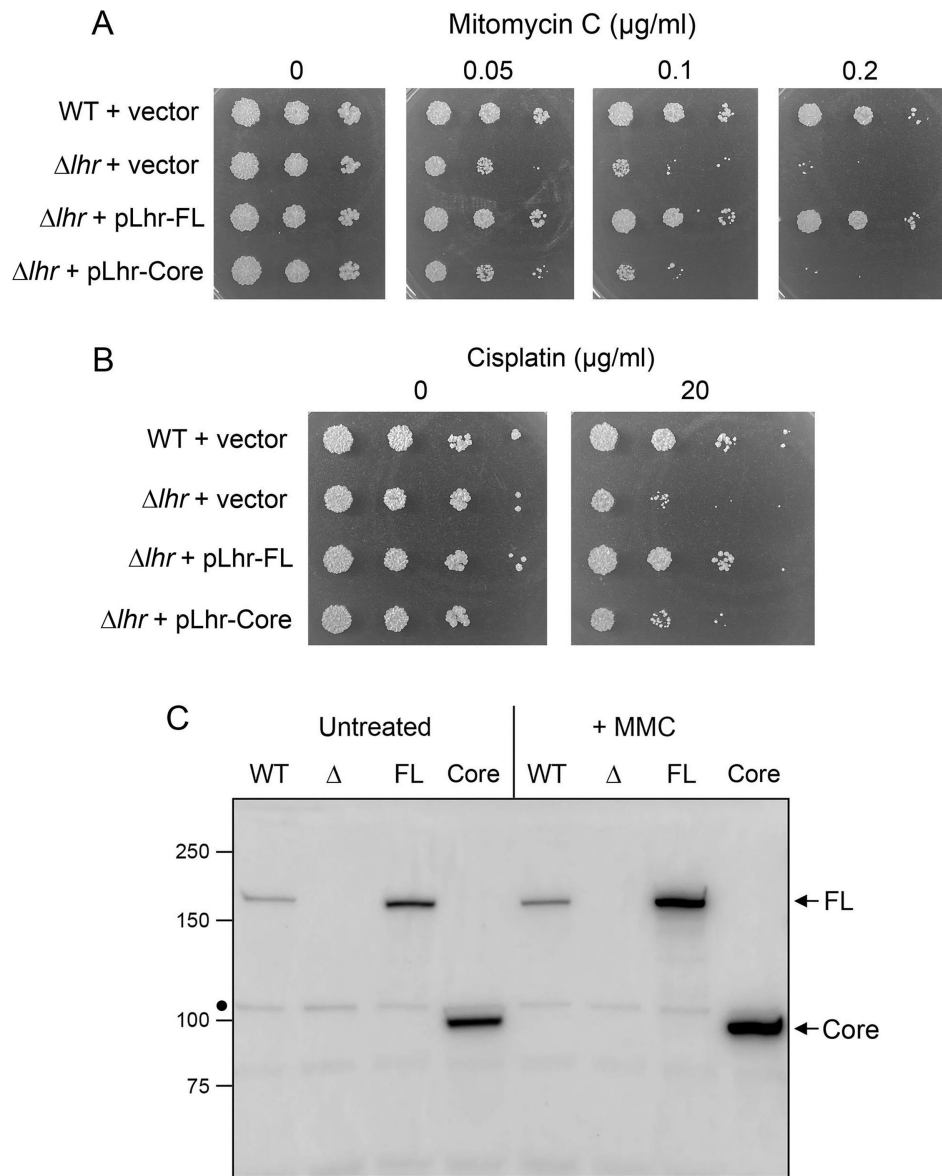


Figure 4. Lhr-CTD is required for MMC and cisplatin resistance. Wild-type and Δlhr strains transformed with plasmids pMV261 (empty vector), pLhr-FL, or pLhr-Core were treated with: (A) 0, 0.05, 0.1, or 0.2 $\mu\text{g/ml}$ MMC for 2 h at 37°C; or (B) 0 or 20 $\mu\text{g/ml}$ cisplatin for 1 h at 37°C. After harvesting and washing to remove clastogen, serial ten-fold dilutions were spotted on 7H10 agar plates containing 20 $\mu\text{g/ml}$ kanamycin to gauge survival. (C) Anti-Lhr Western blot of whole-cell extracts of the indicated strains, harvested before and after MMC treatment. The positions and sizes (kDa) of marker polypeptides are indicated on the left. The positions of immunoreactive full-length (FL) Lhr and Lhr-Core are indicated on the right. A non-specific immunoreactive 105 kDa polypeptide present in all samples (denoted by a black dot on the left) served as a loading control.

verify that no unintended coding changes were acquired during amplification and cloning. The pET21b-Nei2-His6 plasmid was transformed into *E. coli* BL21(DE3) cells. Cultures (4×1 -liter) amplified from a single ampicillin-resistant transformant were grown at 37°C in LB broth containing 100 $\mu\text{g/ml}$ ampicillin until the A_{600} reached 0.7. The cultures were chilled on ice for 1 h, then adjusted to 2% (v/v) ethanol, 10 μM ZnSO_4 , and 0.5 mM isopropyl- β -D-thiogalactopyranoside and incubated for 16 h at 22°C with constant shaking. All subsequent procedures were performed at 4°C. Cells were harvested by centrifugation and resuspended in 80 ml of buffer A (50 mM Tris-HCl, pH 8.0, 500 mM NaCl, 20 mM imidazole, 15 mM β -

mercaptoethanol, 20% glycerol) containing 1 protease inhibitor cocktail tablet (Roche). Lysozyme was added to a concentration of 1 mg/ml. After incubation for 1 h, the resulting lysate was sonicated to reduce viscosity. The insoluble material was pelleted by centrifugation at 38000g for 45 min. The supernatant was mixed for 1 h with 10 ml of Ni-NTA agarose resin (Qiagen) that had been equilibrated with buffer A. The resin was recovered by centrifugation and resuspended in 40 ml of buffer B (50 mM Tris-HCl, pH 8.0, 500 mM NaCl, 20 mM imidazole, 5 mM β -mercaptoethanol, 10% glycerol). The resin was recovered by centrifugation and resuspended in 40 ml of buffer B. This wash step with buffer B was performed three times. The

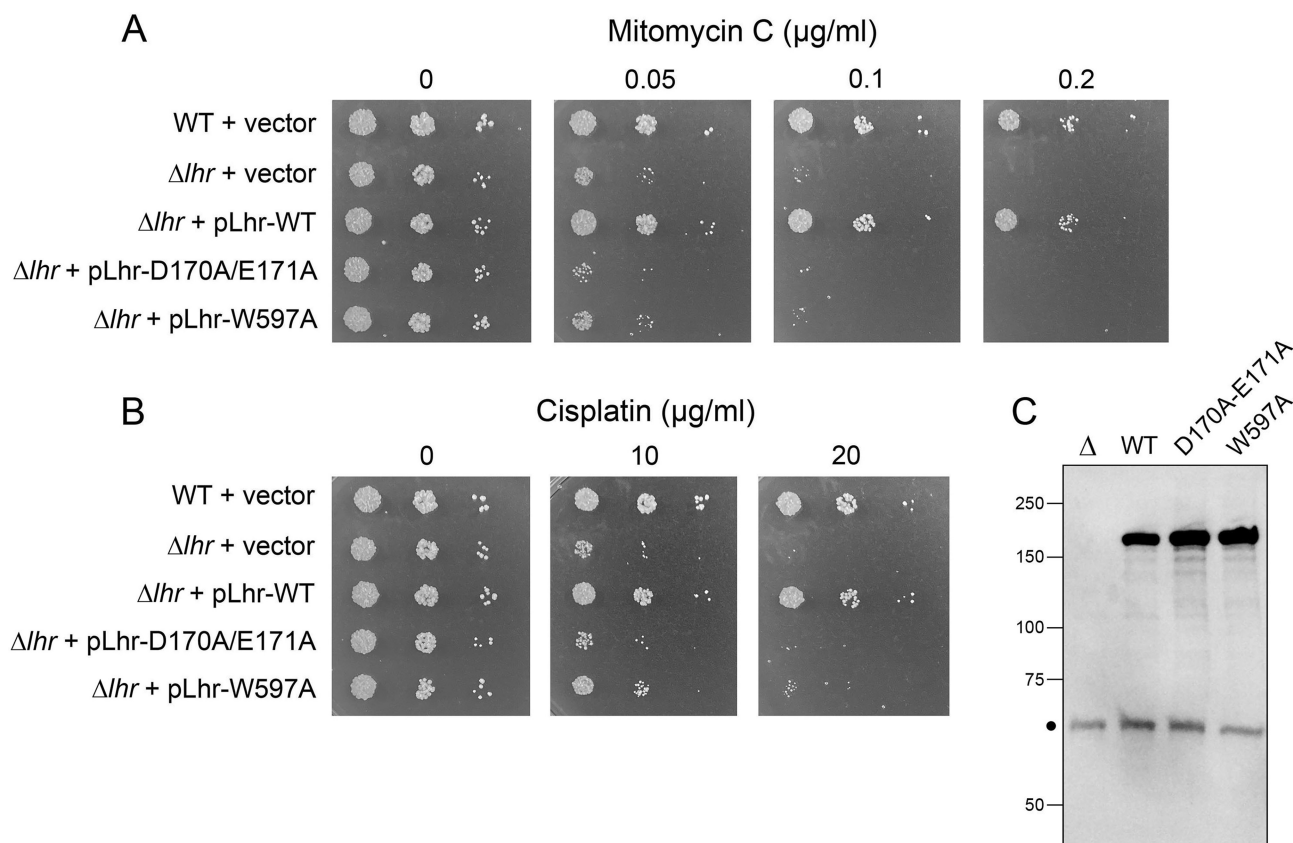


Figure 5. Lhr ATPase and helicase activities are required for MMC and cisplatin resistance. Wild-type and Δlhr strains transformed with plasmids pMV261 (empty vector), pLhr-WT, pLhr-D170A/E171A, or pLhr-W597A were treated with: (A) 0, 0.05, 0.1, or 0.2 $\mu\text{g/ml}$ MMC for 2 h at 37°C; or (B) 0, 10, or 20 $\mu\text{g/ml}$ cisplatin for 1 h at 37°C. After harvesting and washing to remove clastogen, serial 10-fold dilutions were spotted on 7H10 agar plates containing 20 $\mu\text{g/ml}$ kanamycin to gauge survival. (C) Anti-Lhr Western blot of whole-cell extracts of the indicated strains. The positions and sizes (kDa) of marker polypeptides are indicated on the left. A non-specific immunoreactive 65 kDa polypeptide present in all samples (denoted by a black dot on the left) served as a loading control.

thrice-washed resin was poured into a column. After washing the column with 20 ml of buffer B, the bound material was eluted with buffer C (50 mM Tris-HCl, pH 8.0, 500 mM NaCl, 500 mM imidazole, 5 mM β -mercaptoethanol, 10% glycerol). The polypeptide compositions of the eluate fractions were monitored by SDS-PAGE. The eluate fractions containing recombinant Nei2 were pooled, concentrated by centrifugal ultrafiltration, and subjected to gel filtration through a 120-ml Superdex-200 column equilibrated in buffer D (50 mM Tris-HCl, pH 8.0, 500 mM NaCl, 1 mM TCEP, 10% glycerol) while collecting 2-ml fractions. Peak fractions were pooled, concentrated by centrifugal ultrafiltration, frozen, and stored at -80°C . Protein concentrations were determined with the BioRad dye reagent using BSA as the standard. We obtained 4 mg of purified Nei2 per liter of bacterial culture.

RESULTS

Deletion of *lhr* in *M. smegmatis*

In-frame deletion of the entire open reading frame (ORF) of *lhr* (spanning aa 1–1507) in *M. smegmatis* mc²155 was achieved by two-step allelic exchange with selectable and counterselectable markers (14). In this way, we min-

imized risk of a potential polar effect on expression of the 3'-flanking *nei2* gene (Figure 2A). The Δlhr mutant grew as well as the wild-type strain in liquid culture in 7H9 medium, with doubling times of 155 and 156 min, respectively.

Deletion of *lhr* sensitizes *M. smegmatis* to killing by MMC and cisplatin

Mitomycin C (MMC) reacts with guanine bases at 5'-CpG sites to form inter-strand G-G crosslinks and G-monoadducts via reaction with guanine-N2 in the DNA minor groove (16). In light of previous reports (6–9) that *lhr* is upregulated in mycobacteria exposed to MMC, we interrogated the sensitivity of Δlhr cells to killing by MMC in comparison to wild-type *M. smegmatis*. Logarithmically growing cultures were mock-treated or exposed to 0.05, 0.1, or 0.2 $\mu\text{g/ml}$ MMC for 2 h. Cells were then harvested, washed to remove residual MMC, and serial 10-fold dilutions were spotted on 7H10 agar plates to gauge survival. The Δlhr strain suffered a ~ 10 -fold reduction in survival after exposure to 0.05 $\mu\text{g/ml}$ MMC and a 100-fold reduction after exposure to 0.1 $\mu\text{g/ml}$ MMC, doses that had virtually no effect on wild-type *M. smegmatis* (Figure 2B). Δlhr cells were ~ 100 -fold more sensitive than wild-

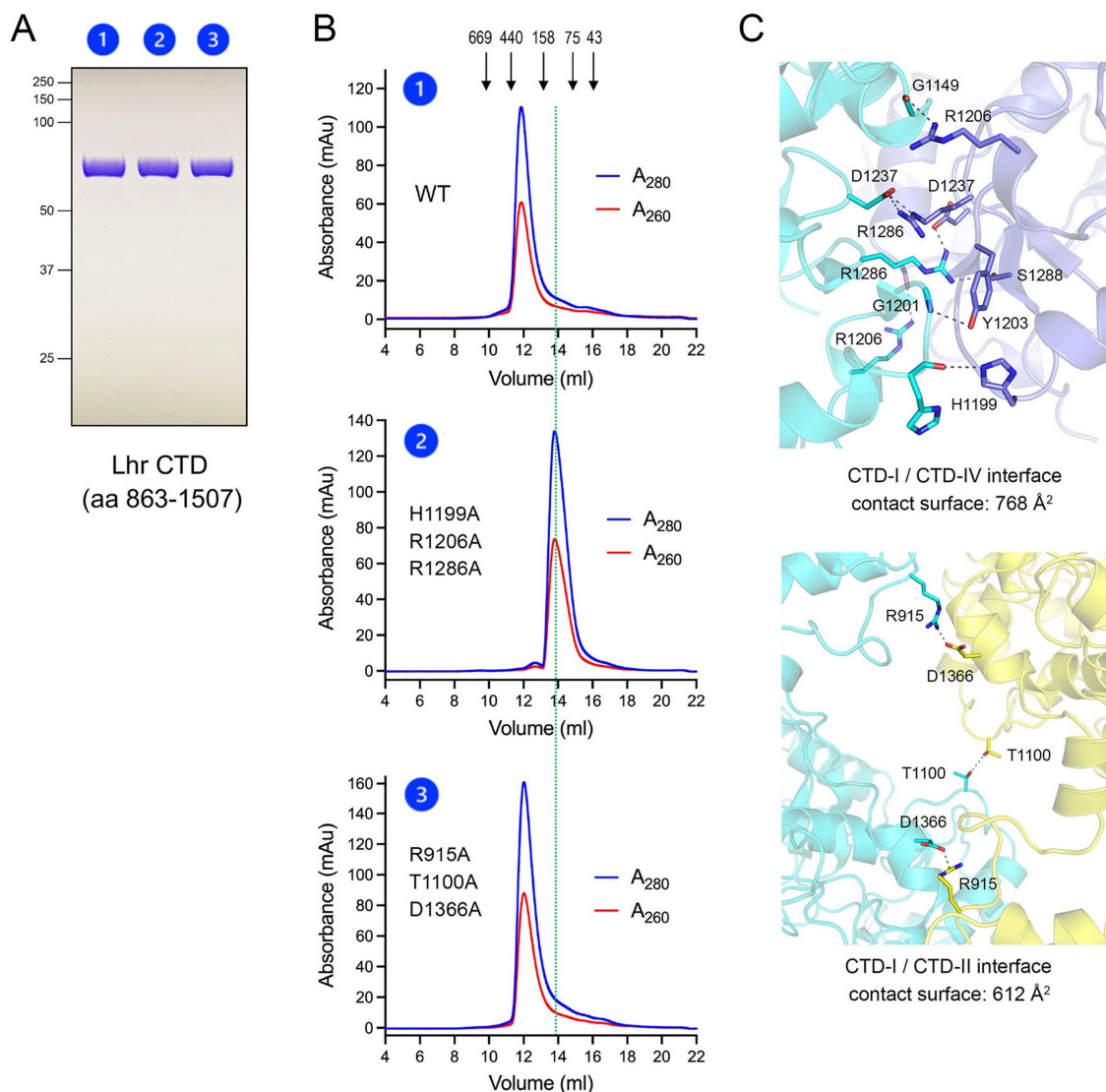


Figure 6. Mutational interdiction of CTD tetramerization. (A) Aliquots (5 μ g) of recombinant wild-type Lhr-CTD (lane 1) and CTD mutants H1199A-R1206A-R1286A (lane 2) and R915A-T1100A-D1366A (lane 3) were analyzed by SDS-PAGE. The Coomassie blue-stained gel is shown. The positions and sizes (kDa) of marker polypeptides are indicated on the left. (B) Aliquots of wild-type CTD (0.5 ml, 0.3 mg/ml; panel 1), and mutants H1199A-R1206A-R1286A (0.5 ml, 0.3 mg/ml; panel 2) and R915A-T1100A-D1366A (0.5 ml, 0.5 mg/ml; panel 3) were gel filtered through a 24-ml Superdex-200 column equilibrated with 50 mM HEPES-NaOH, pH 7.5, 300 mM KCl, 1 mM DTT, 10% glycerol. The elution profiles were monitored continuously by A_{280} (blue curve) and A_{260} (red curve) as a function of elution volume. Arrows above panel 1 denote the elution peaks and native sizes for a mixture of calibration standards: thyroglobulin (669 kDa), ferritin (440 kDa), aldolase (158 kDa), conalbumin (75 kDa), and ovalbumin (44 kDa). (C) Atomic contacts (dashed lines) at the interface of homo-tetramer subunits CTD-I (cyan) and CTD-IV (blue) (top panel) and of subunits CTD-I (cyan) and CTD-II (yellow) (bottom panel).

type to killing by 0.2 μ g/ml MMC (Figure 2B). An *M. smegmatis* Δ uvrD1 strain lacking the nucleotide excision repair (NER) helicase UvrD1, which has a mild growth defect and hence forms smaller colonies (15), displays sensitivity to 0.05 μ g/ml MMC similar to that of Δ lhr and was slightly less sensitive than Δ lhr to 0.1 and 0.2 μ g/ml MMC (Figure 2B). A Δ lhr Δ uvrD1 double-mutant was \sim 10-fold more sensitive to killing by 0.05 μ g/ml MMC than either of the single mutants (Figure 2B), suggesting that Lhr and UvrD1 participate in parallel pathways of MMC damage repair.

Cisplatin forms intra-strand G-G and G-A crosslinks, inter-strand G-G crosslinks, and G-monoadducts via re-

action with purine-N7 in the major groove (17). Wild-type, Δ lhr, Δ uvrD1, and Δ lhr Δ uvrD1 cells were mock-treated or exposed to cisplatin for 1 h, then harvested, washed, and spotted in serial 10-fold dilutions on 7H10 agar plates to gauge survival. Δ lhr cells were \sim 10-fold and \geq 100-fold more sensitive than wild-type to killing by 10 and 20 μ g/ml cisplatin (Figure 2C). Δ lhr Δ uvrD1 double-mutant cells were more sensitive to 10 μ g/ml cisplatin than the Δ lhr strain and the Δ lhr Δ uvrD1 double-mutant was even more sensitive to 10 μ g/ml cisplatin than the Δ uvrD1 strain, implying that Lhr and UvrD1 are engaged in parallel pathways of cisplatin damage repair. (Figure 2C).

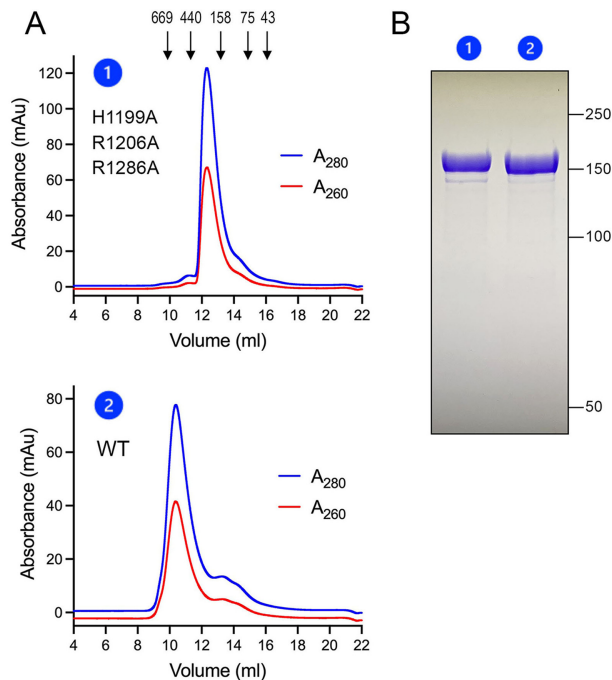


Figure 7. H1199A-R1206A-R1286A interdicts tetramerization of full-length Lhr. (A) Recombinant full-length H1199A-R1206A-R1286A mutant (0.5 ml, 0.4 mg/ml; panel 1) and full-length wild-type Lhr (0.5 ml, 0.2 mg/ml; panel 2) were gel filtered through a 24-ml Superdex-200 column equilibrated with buffer containing 50 mM HEPES–NaOH, pH 7.5, 300 mM KCl, 1 mM DTT, 10% glycerol. The elution profiles were monitored continuously by A_{280} and A_{260} as a function of elution volume. Arrows denote the elution peaks and native sizes for a mixture of calibration standards: thyroglobulin (669 kDa), ferritin (440 kDa), aldolase (158 kDa), conalbumin (75 kDa), and ovalbumin (44 kDa). (B) Aliquots (5 μ g) of the peak Superdex fractions of full-length H1199A-R1206A-R1286A mutant (lane 1) and full-length wild-type Lhr (lane 2) were analyzed by SDS-PAGE. The Coomassie blue-stained gel is shown. The positions and sizes (kDa) of marker polypeptides are indicated on the right.

lhr deletion does not sensitize *M. smegmatis* to killing by MMS or UV irradiation

Ultraviolet radiation causes two classes of intra-strand DNA lesions—cyclobutane pyrimidine dimers and 6–4 photoproducts—that are repaired in *M. smegmatis* via NER, as evinced by the exquisite sensitivity of Δ *uvrD1* cells to killing by UV irradiation (15). To query whether the Δ *lhr* mutant is UV sensitive, we spotted serial dilutions of wild-type and Δ *lhr* cells on 7H10 agar plates, along with Δ *uvrD1* cells (as a positive control for enhanced UV killing). The plates were then mock-treated or exposed to escalating doses (1, 5, or 10 mJ/cm²) of 254 nm UV light. Following treatment, the plates were wrapped in foil (to prevent repair by photolyase) and incubated at 37°C. The wild-type and Δ *lhr* strains were equally resistant to 1 and 5 mJ/cm² and modestly sensitive to 10 mJ/cm², while the Δ *uvrD1* strain suffered a ~10-fold reduction in survival at 1 mJ/cm² and a >100-fold reduction in survival at 5 mJ/cm² (Figure 3A). It is noteworthy that the Δ *lhr* Δ *uvrD1* double-mutant was no more sensitive to UV than the Δ *uvrD1* single mutant.

Methyl methanesulfonate (MMS) is a DNA alkylating agent that generates 7-methyl-G and 3-

methyl-A base monoadducts. We found that wild-type and Δ *lhr* cells were equally sensitive to killing by 1 h treatments with 0.1, 0.2, and 0.4% MMS (Figure 3B).

What features of Lhr are needed for its role in MMC and cisplatin damage repair *in vivo*?

Having established two DNA repair phenotypes elicited by the absence of Lhr, we focused henceforth on determining which of the several biochemical activities and physical properties of Lhr are pertinent to its *in vivo* functions. To wit: (i) is ATP hydrolysis necessary? (ii) is DNA unwinding necessary? (iii) is the CTD necessary, or is the helicase core sufficient? (iv) if the CTD is necessary, why is it necessary? To answer these questions, we sought to complement the MMC and cisplatin sensitivity of Δ *lhr* cells by expression of wild-type Lhr and biochemically defined mutant Lhr proteins. Our approach was to express the potentially complementing Lhr proteins from a kanamycin-resistance plasmid under the control of the native *lhr* promoter. To validate the complementation assay, *M. smegmatis* wild-type and Δ *lhr* strains were transformed with pLhr-FL (expressing full-length wild-type Lhr) or the empty vector, and transformants were tested for MMC sensitivity. We saw that pLhr-FL restored a ‘wild-type’ MMC resistance phenotype (Figure 4A). Expression of the plasmid-encoded Lhr-FL protein was affirmed by Western blotting of protein of whole-cell extracts of the untreated and MMC-treated transformant with affinity-purified anti-(Lhr-FL) antibody (Figure 4C). Three key points are apparent from the immunoblot: (i) that the antibody recognized a ~180 kDa polypeptide in wild-type cells that is absent in the Δ *lhr* mutant; (ii) that Δ *lhr* cells harboring pLhr-FL express higher steady-state levels of Lhr than wild-type cells bearing the empty vector, reflecting increased *lhr* gene dosage on the plasmid versus the mycobacterial chromosome; (iii) that MMC treatment increases the steady-state level of the Lhr protein, in keeping with prior evidence that *lhr* mRNA levels increase after MMC treatment (6–9). We proceeded to validate the complementation assay for cisplatin damage repair, whereby introducing pLhr-FL into Δ *lhr* cells restored a ‘wild-type’ cisplatin resistance phenotype (Figure 4B).

The CTD is essential for MMC and cisplatin resistance: helicase core does not suffice

Lhr-Core (aa 1–856) is a monomeric DNA-dependent ATPase-helicase (1–3). To query its biological activity, we transformed the Δ *lhr* strain with pLhr-Core. Western blotting verified that: (i) the 100 kDa Lhr-Core protein was expressed at steady-state level similar to that of full-length Lhr and (ii) Lhr-Core expression increased upon treatment with MMC (Figure 4C). However, Lhr-Core expression failed to restore MMC or cisplatin resistance, i.e. Δ *lhr* cells bearing pLhr-Core were as sensitive to killing by MMC and cisplatin as Δ *lhr* cells carrying the empty vector (Figure 4A and B). We conclude that the CTD is essential for Lhr function in abetting MMC and cisplatin resistance.

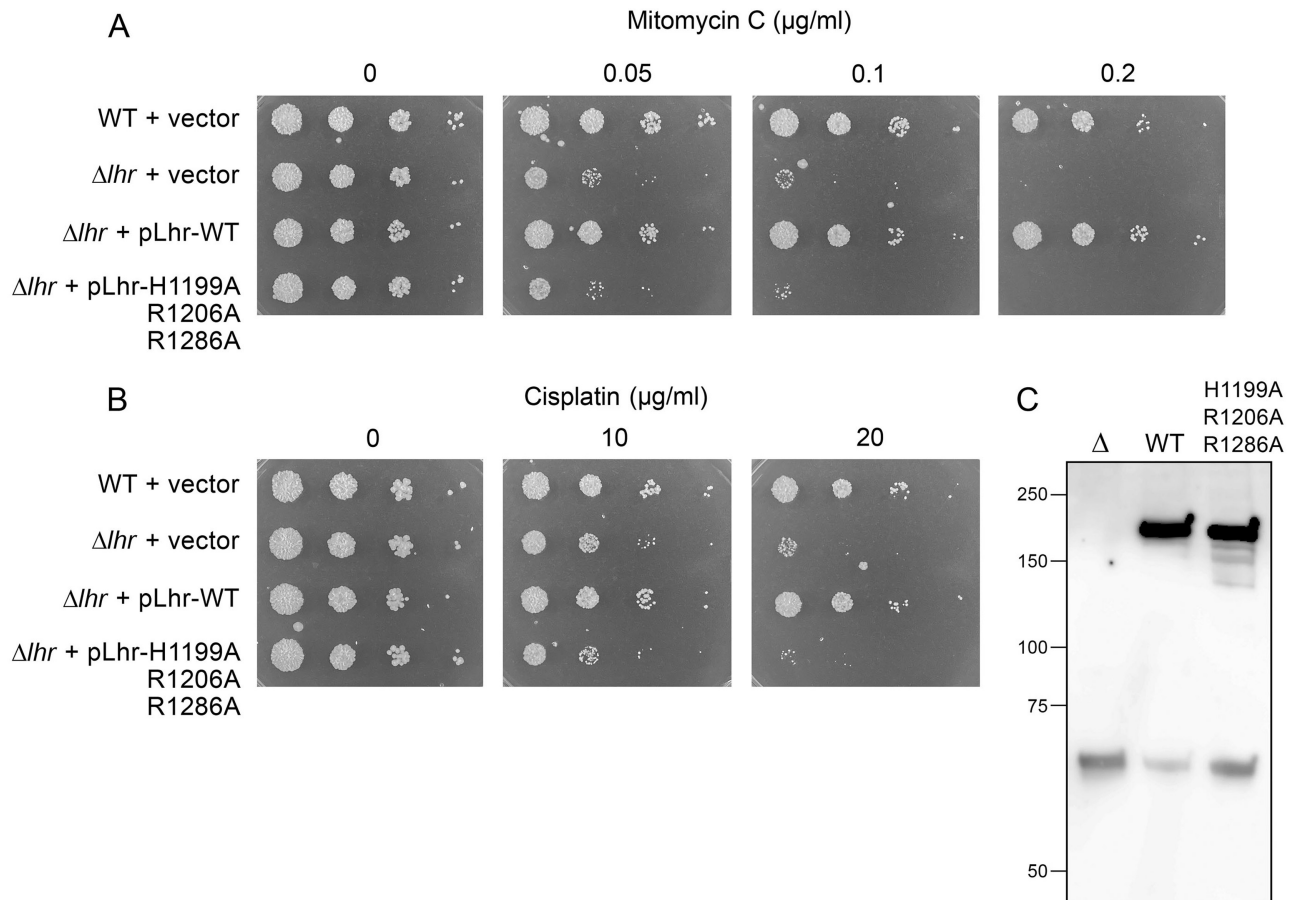


Figure 8. Lhr tetramerization is required for MMC and cisplatin resistance. Wild-type and Δlhr strains transformed with plasmids pMV261 (vector), pLhr-WT, or pLhr-H1199A-R1206A-R1286A were treated with: (A) 0, 0.05, 0.1, or 0.2 $\mu\text{g/ml}$ MMC for 2 h at 37°C or (B) 0, 10, or 20 $\mu\text{g/ml}$ cisplatin for 1 h at 37°C. After harvesting and washing to remove clastogen, serial ten-fold dilutions were spotted on 7H10 agar plates containing 20 $\mu\text{g/ml}$ kanamycin to gauge survival. (C) Anti-Lhr Western blot of whole-cell extracts of the indicated strains. The positions and sizes (kDa) of marker polypeptides are indicated on the left.

Lhr ATPase and helicase activities are required for MMC and cisplatin resistance

Lhr is a member of the DExH-box clade of superfamily II NTPase/helicase enzymes, so-named for the signature DExH peptide motif (also called motif II, or Walker B box) that coordinates the divalent cation cofactor for NTP hydrolysis (2). Mutating Lhr motif II $^{170}\text{DEVH}^{173}$ to $^{170}\text{AAVH}^{173}$ will abolish ATPase activity, and consequently helicase activity. To test whether ATP hydrolysis is required for Lhr function in DNA repair, Δlhr cells were transformed with pLhr-D170A/E171A expressing the full-length motif II mutant. Structure-guided mutagenesis of the Lhr interface identified Trp597 as essential for coupling ATP hydrolysis to mechanical work (2). The Trp597 indole stacks on a tracking strand nucleobase that is thought to demarcate the single-strand:double-strand junction of the helicase substrate (Figure 1B). Mutating Trp597 to alanine abolished Lhr helicase activity without affecting DNA-dependent ATPase activity (2). To test whether helicase activity is required for Lhr function, Δlhr cells were transformed with pLhr-W597A. Western blotting confirmed that both full-length mutant proteins were expressed at levels

comparable to wild-type Lhr (Figure 5C). However, neither Lhr mutant was able to complement the MMC or cisplatin sensitivity of the Δlhr strain (Figure 5A and B). Thus, the helicase activity is necessary for Lhr function *in vivo* and ATP hydrolysis uncoupled from motor activity does not suffice.

Is tetrameric quaternary structure nucleated by the CTD essential for Lhr activity *in vivo*?

Having established that deletion of the CTD eliminates Lhr's repair activity *in vivo* (Figure 4), we envisioned two ways in which the CTD might contribute: (i) by enforcing a homo-tetrameric quaternary structure of Lhr that is necessary for biological activity or (ii) by performing an essential repair task unrelated to CTD tetramerization. We aimed to flesh out these models by: (i) introducing mutations at the subunit interfaces of the CTD tetramer so as to identify variants that form only homodimers or monomers; (ii) introduce interface-disrupting mutations into full-length Lhr and (iii) test biochemically validated mutants for DNA repair activity *in vivo*.

The cryo-EM structure of the CTD tetramer highlighted cross-protomer contacts at the subunit interfaces (3). The contact surfaces formed by CTD-I and CTD-IV and (pseudo symmetry-related) CTD-II and CTD-III (Figure 1C) are the main subunit interfaces. The inter-subunit contacts are mainly via hydrogen bonds or salt bridges between Arg1206 and Gly1149-O, Arg1286 and Asp1237, Ser1288 and Arg1286, Tyr1203 and Gly1201-N, and His1199-Ne and His1199-O (Figure 6C). To potentially interdict this interface, we produced recombinant Lhr-CTD (aa 863–1507) in which His1199, Arg1206 and Arg1286 were mutated to alanine (Figure 6A). Additional interfaces are formed by CTD-I and CTD-II and (pseudo symmetry-related) CTD-III and CTD-IV (Figure 1C), wherein Asp1366 makes a salt bridge to Arg915, a hydrogen bond is made between the Ala917 amide and the Gly1314 carbonyl, and Thr1100 makes a hydrogen bond to Thr1100 in the neighbor protomer (Figure 6C). To tweak this interface, we produced recombinant Lhr-CTD in which Arg915, Thr1100, and Asp1366 were mutated to alanine (Figure 6A). The wild-type CTD and the two interfacial mutants were analyzed by gel filtration chromatography (Figure 6B). Wild-type CTD and the R915A-T1100A-D1366A mutant gel filtered as single components with elution volumes corresponding to a homo-tetramer. By contrast, the H1199A-R1206A-R1286A CTD mutant eluted as a single component at a volume consistent with a dimeric quaternary structure (Figure 6B).

The disruptive H1199A-R1206A-R1286A triple mutation was introduced into full-length Lhr and the recombinant protein was analyzed by gel filtration in parallel with full-length wild-type Lhr. Here, too, the H1199A-R1206A-R1286A mutation elicited a shift toward later elution volume vis-à-vis the wild-type Lhr homo-tetramer (Figure 7).

Having affirmed mutational interdiction of tetramerization, we tested the ability of Lhr-(H1199A-R1206A-R1286A) expression to complement the DNA damage sensitivities of Δ lhr. Western blotting indicated that wild-type and H1199A-R1206A-R1286A Lhr proteins were expressed at equivalent levels (Figure 8C). The instructive finding was that the H1199A-R1206A-R1286A mutant failed to restore MMC or cisplatin resistance (Figure 8A and B). We conclude that tetramerization is a key function of the Lhr-CTD in DNA damage repair *in vivo*, i.e. that full-length Lhr with less than tetrameric quaternary structure does not suffice.

We proceeded to compare the RNA:DNA and DNA:DNA helicase activities of purified full-length wild-type Lhr and the full-length H1199A-R1206A-R1286A mutant. The helicase assay format entailed preincubation of Lhr with a 3'-tailed substrate consisting of a 24-bp RNA:DNA or DNA:DNA duplex with a 20-mer 3' DNA tail to serve as a loading strand (Figure 9). Unwinding was initiated by addition of ATP, with simultaneous addition of a 40-fold excess of unlabeled 24-mer displaced strand. The unlabeled trap strand minimizes reannealing of any radiolabeled 24-mer that was unwound by Lhr and it competes with the loading strand for binding to any free Lhr that dissociated from the labeled 3'-tailed duplex without unwinding it. Lhr titration experiments showed that: (i) the wild-type and H1199A-R1206A-R1286A

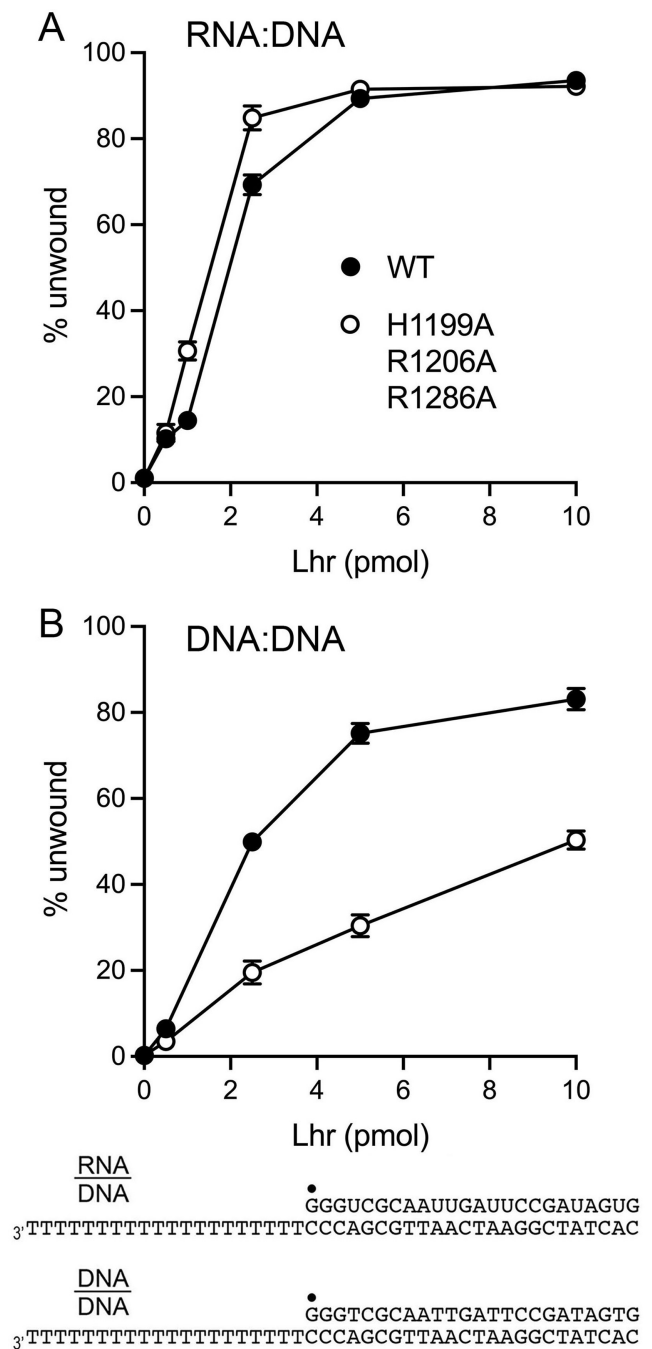


Figure 9. Effect of H1199A-R1206A-R1286A mutation on Lhr helicase activity. Reaction mixtures (10 μ l) containing 20 mM Tris-HCl, pH 7.0, 150 mM NaCl, 1 mM DTT, 5 mM CaCl₂, 0.5 pmol (50 nM) ³²P-labeled 3'-tailed duplex nucleic acid as specified—either RNA:DNA (panel A) or DNA:DNA (panel B), and 0.5, 1, 2.5, 5, or 10 pmol (0.05, 0.1, 0.25, 0.5, or 1 μ M) wild-type or H1199A-R1206A-R1286A mutant Lhr as specified were preincubated for 10 min at room temperature. The unwinding reactions were initiated by adding 1 mM ATP and a 40-fold excess of an unlabeled 24-mer DNA oligonucleotide identical to the labeled strand of the DNA helicase substrate. The reaction mixtures were incubated for 30 min at 37°C and then quenched by adding 1 μ l of a solution containing 5% SDS, 100 mM EDTA. The mixtures were supplemented with 4 μ l of 70% glycerol, 0.3% bromophenol blue. The reaction products were analyzed by electrophoresis through a 15-cm 12% polyacrylamide gel in 89 mM Tris-borate, 2.5 mM EDTA. The extents of duplex unwinding were quantified by scanning the gel. Each datum is the average of three independent Lhr titration experiments \pm SEM.

enzymes were equally adept at unwinding the RNA:DNA hybrid (Figure 9A) and (ii) the specific activity of H1199A-R1206A-R1286A in DNA:DNA unwinding was half that of wild-type Lhr (Figure 9B). We surmise that tetramerization enhances, but is not required for, Lhr's DNA helicase activity.

Might Nei2 contribute to an Lhr pathway of crosslink repair?

Based on the genetic evidence presented above, we envision that Lhr anchors a novel mycobacterial pathway of DNA crosslink repair, populated by additional enzymes and proteins that remain to be identified. Likely candidates might include: (i) a glycosylase that ejects an MMC- or cisplatin-adducted guanine nucleobase to leave an abasic site; (ii) a nuclease that incises at sites flanking the crosslink; and/or (iii) a bypass or gap-filling polymerase. Three considerations lead us to speculate that Lhr cooperates with a glycosylase during inter-strand crosslink repair. First, the Lhr-CTD is structurally homologous to AlkZ, a DNA glycosylase that dismantles the inter-strand guanine crosslinks generated by the bacterial toxin Azinomycin B (3,5,18). However, at present, there is no evidence that Lhr-CTD has a glycosylase activity. Moreover, the putative active site residues of AlkZ are not conserved in Lhr and the counterpart of a predicted DNA-binding site of AlkZ is buried within the Lhr-CTD tetramer and thus inaccessible to DNA. Second, the eukaryal glycosylase NEIL3 catalyzes unhooking of inter-strand psoralen and abasic site crosslinks *in vivo* and *in vitro* (19–21). Third, and most compelling, is the fact that *lhr* is the upstream ORF in a two-gene mycobacterial operon that includes *nei2* (Figure 2A). *lhr* and *nei2* are coordinately transcriptionally upregulated in response to DNA damage (6–11), implying they might be linked functionally. *M. smegmatis* Nei2 is a 252-aa polypeptide named for its homology to *E. coli* endonuclease VIII (Nei), a bifunctional repair enzyme with DNA glycosylase and AP lyase activities (22). Nei/Fpg-type glycosylases exploit the secondary amino group of an N-terminal proline residue (corresponding to Pro2 of the *nei*-encoded polypeptide) as a nucleophile that attacks the deoxyribose C1' of the target nucleoside, leading to expulsion of the nucleobase and formation of a covalent Nei-DNA Schiff base intermediate (which can be trapped in the presence of NaBH₄) (22,23). The AP lyase activity then executes either one β -elimination step or a β -elimination step followed by a δ -elimination step to incise the DNA backbone. Despite the suggestive homology, there are conflicting reports in the literature on what activities, if any, are inherent to Nei2. For example, the Wallace lab produced and purified recombinant *M. tuberculosis* Nei2 with a C-terminal His-tag and found it to be enzymatically inactive (i.e. less than 1% of the recombinant Nei2 was able to form a borohydride-trappable DNA adduct) (24). In contrast, the Ramachandran lab produced recombinant Nei2 fused to an N-terminal GST tag and purified the protein via adsorption to glutathione-agarose and elution with glutathione, which yielded a mixture of GST-Nei2, free GST, and other polypeptides (25). Further purification by gel filtration yielded a peak of GST-Nei2 that was construed to comprise a homo-octamer of the GST-Nei2 polypeptide (25). A later publication by the same group stated that pu-

rified GST-Nei2 eluted during gel filtration as a dodecamer (26). (Because the GST tag per se will drive homodimerization of any GST fusion protein, these gel filtration results are not indicative of the native size of Nei2.) They reported that the GST-Nei2 protein had glycosylase and lyase activities on single-strand or duplex DNA substrates containing a single uracil or 5-hydroxyuracil deoxynucleosides. Moreover, GST-Nei2 was reportedly active in cleaving DNA containing a single THF (tetrahydrofuran) abasic site (25,26). Such activity is surprising given that the N-terminal GST tag ought to preclude nucleophilic attack by the (now internally positioned) proline of Nei2.

Characterization of *M. smegmatis* Nei2

To address these discrepancies regarding mycobacterial Nei2, we produced the *M. smegmatis* protein in *E. coli* as a C-terminal His₆-fusion and purified it from a soluble extract via sequential Ni-agarose chromatography and preparative gel filtration steps. The 29-kDa Nei2 protein gel-filtered as a single component (Figure 10A). The peak fraction was subjected to a second round of analytical gel filtration, in parallel with a mixture of size standards, which revealed that Nei2 eluted a volume consistent with a monomeric native molecular size (Figure 10B). To test for AP lyase activity, we exploited a 24-mer 5' ³²P-labeled DNA oligonucleotide containing a single centrally placed uracil nucleoside that was pretreated with *E. coli* uracil DNA glycosylase (UDG) to generate an abasic site. Ensuing reaction of 2 pmol of abasic DNA with Nei2 at 37°C resulted in DNA incision, whereby the yield of cleaved product was proportional to input Nei2 and was quantitative at 1 pmol of Nei2 (Figure 11A). Cleavage of dU-containing DNA by 4 pmol Nei2 was dependent on pretreatment of the substrate with UDG (Figure 11A). An otherwise identical UDG-treated dT-containing substrate was refractory to cleavage by Nei2 (Figure 11A). Incubation of the UDG-pretreated abasic DNA (2 pmol) with Nei2 in the presence of 50 mM NaBH₄ resulted in the trapping of a covalent Nei2-DNA adduct that was detectable by SDS-PAGE, with the extent of adduct formation being proportional to input Nei2 and saturating at ≥ 10 pmol of Nei2 with 87% of the DNA being attached to Nei2 (Figure 11B). An additional product, migrating during SDS-PAGE slightly ahead of the input 24-mer DNA, corresponds to DNA cleaved by Nei2 that eluded trapping by borohydride at the Schiff base intermediate step. (From the fact that 4 pmol of Nei2 resulted in trapping 0.8 pmol of abasic DNA, we surmise that at least 20% of the Nei2 protein preparation is active as an AP lyase.)

We tracked the kinetics of Nei2-DNA adduct formation at 22°C in reactions containing a 5-fold molar excess of Nei2 over DNA (Figure 12A). An endpoint at which 78% of the input ³²P-DNA was covalently attached to Nei2 was attained in 90 to 120 s. Fitting the data to a one-phase association model in Prism yielded an apparent rate constant of $2.95 \pm 0.12 \text{ min}^{-1}$ for formation of the Schiff base intermediate (Figure 12B). A parallel analysis under the same conditions, albeit in the absence of borohydride, illuminated the kinetics of DNA cleavage (Figure 12C). We derived an apparent rate constant of $3.12 \pm 0.24 \text{ min}^{-1}$ for the com-

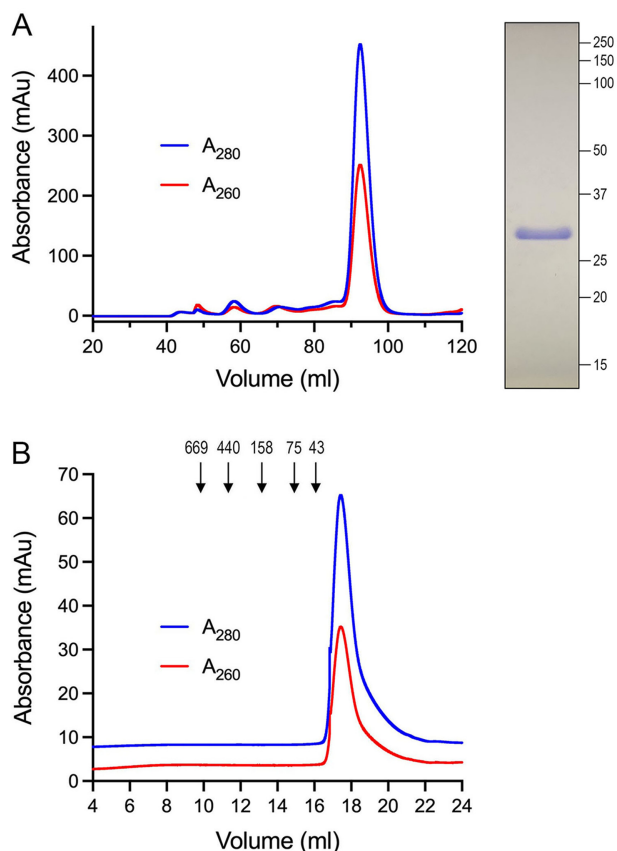


Figure 10. Nei2 is a monomeric protein. (A) Preparative gel filtration of the Ni-agarose fraction of Nei2 through a 200-ml Superdex-200 column was performed as described under Methods. The elution profile was monitored continuously by A_{280} and A_{260} as a function of elution volume. An aliquot (5 μ g) of the peak fraction was analyzed by SDS-PAGE. The Coomassie blue-stained gel is shown. The positions and sizes (kDa) of marker polypeptides are indicated. (B) Analytical gel filtration. An aliquot (0.5 ml, 0.2 mg/ml) of the peak Nei2 fraction from the column in panel A was gel filtered through a 24-ml Superdex-200 column equilibrated with buffer containing 50 mM Tris-HCl, pH 8.0, 500 mM NaCl, 1 mM TCEP, 10% glycerol. The elution profile was monitored continuously by A_{280} and A_{260} as a function of elution volume. Arrows denote the elution peaks and native sizes for a mixture of calibration standards.

posite AP lyase reaction. Given that the rate of the initial step of Schiff base formation was virtually the same as that of the overall lyase reaction, we surmise that the Schiff base formation is rate-limiting for incision by Nei2 at an abasic site.

To gauge whether Nei2 was active on duplex DNA, we annealed the 24-mer 5'- 32 P-labeled dU-containing DNA oligonucleotide to a complementary unlabeled 24-mer DNA and isolated the blunt-end 24-bp duplex by preparative native gel electrophoresis. (Analytical native PAGE affirmed that the radiolabeled strand was in a duplex form that migrated more slowly than the labeled single strand.) A 5-fold molar excess of Nei2 was reacted with the 24-duplex DNA that had been pretreated with UDG under the same conditions employed for the UDG-treated abasic single-stranded 24-mer in Figure 12C. The salient finding was that Nei2 was ineffective as an AP lyase on duplex DNA, cleaving only 5% of the input abasic strand of the duplex 24-mer

versus 90% of the single-strand substrate after a 2 min incubation under single turnover conditions (Figure 12C).

To affirm the outcome of the Nei2 lyase reaction, we analyzed in parallel the cleavage product formed after Nei2 incubation with UDG-pretreated dU substrate to the species generated by treatment of the UDG-pretreated dU substrate with alkali. The latter treatment generates a mixture of two 5'- 32 P-labeled DNA fragments: a slower migrating species formed by β elimination and a faster migrating species (3'-monophosphate-terminated) that underwent sequential β and δ eliminations. The predominant outcome of the Nei2 reaction was β elimination (Figure 12D).

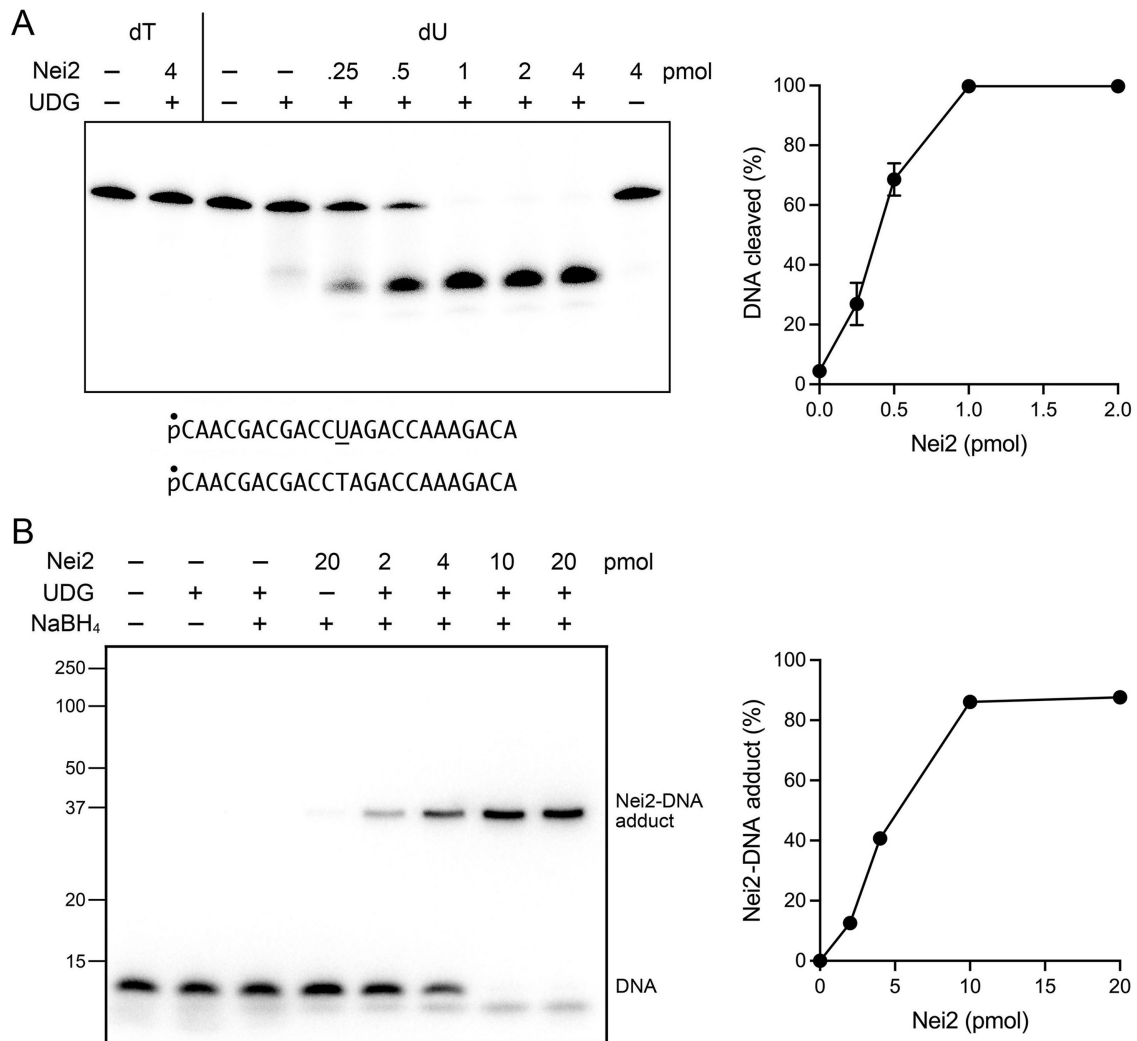
We proceeded to test whether Nei2 could incise a 24-mer 5'- 32 P-labeled DNA oligonucleotide containing a single THF abasic site and found that no cleavage of the THF DNA was detectable in the presence of input Nei2 that sufficed to completely cleave UDG-pretreated abasic DNA (Figure 13A). Nei2 failed to form a protein-DNA adduct when reacted with THF DNA under conditions of enzyme excess (Figure 13B).

DNA glycosylase activity was tested by reaction of Nei2 with 1 pmol of dU-containing single-strand DNA that had not been pretreated with UDG. Because preliminary experiments indicated that detectable incision of the dU substrate (entailing sequential glycosylase and lyase steps) required a large molar excess of Nei2 (the extent of cleavage at pH 8.5 was proportional to input Nei2 between 25 and 100 pmol, with 15% of DNA cleaved at 100 pmol Nei2), we varied the pH of the reaction mixture in search of optimal conditions. Cleavage of 1 pmol of dU-containing DNA by 100 pmol of Nei2 was optimal at pH 8.5 to 9.5 and declined steadily at lower pH values (Figure 14). At the pH optimum, one-sixth of the input DNA was incised to yield a predominant product of β elimination by lyase at the abasic site formed by the glycosylase and a minor, faster migrating product of β and δ elimination. Reaction of 100 pmol of Nei2 with 1 pmol of dU-containing 24-bp duplex DNA that had not been pretreated with UDG resulted in cleavage of <1% of the input 32 P-labeled strand (not shown). Our findings run counter to the report that GST-Nei2 was equally active as a glycosylase/lyase on single-strand and duplex dU-containing DNA substrates (25).

DISCUSSION

The present study extends our understanding of the physiology of mycobacterial Lhr in several key respects. We demonstrate that absence of Lhr elicits sensitivity to bacterial killing by two different DNA crosslinking agents, MMC and cisplatin, that form covalent adducts in the DNA minor groove and major groove, respectively, leading to a mixed spectrum of inter-strand crosslinks, intra-strand crosslinks, and monoadducts. Lhr deletion does not impact mycobacterial sensitivity to two other clastogens: MMS, which forms alkylpurine monoadducts; and UV radiation, which generates intra-strand thymine dimers. A parsimonious interpretation is that Lhr specializes in the repair of inter-strand crosslinks.

Our results suggest a division of labor between Lhr and UvrD1 in dealing with DNA adducts. In keeping with its function as an agent of NER, UvrD1 is critical for re-



sistance to UV damage (15,27), a pathway in which Lhr plays no discernable role. Yet, both Lhr and UvrD1 contribute to protecting *M. smegmatis* from killing by MMC and cisplatin, the instructive finding being that a Δ lhr Δ uvrD1 double-mutant is more sensitive to MMC and cisplatin than either single mutant. We envision that UvrD1-dependent NER is responsible for rectifying MMC and cisplatin monoadducts and intra-strand crosslinks, whereas Lhr aids the repair of MMC and cisplatin inter-strand crosslinks.

We conducted a series of Δ lhr complementation assays with biochemically defined Lhr mutants to gauge which ac-

tivities and structural properties of Lhr are pertinent to its activity *in vivo*. It was not a foregone conclusion that the effects of deleting Lhr protein would be synonymous with those of interdicting either its ATPase or helicase activities. The caveat to such assumptions is exemplified by the genetic and biochemical analyses of mycobacterial UvrD2 helicase. The UvrD2 protein is essential for viability of *M. smegmatis* and *M. tuberculosis*, i.e. attempts to disrupt the *uvrD2* gene were unsuccessful unless a second copy of *uvrD2* was present elsewhere in the chromosome (28,29). UvrD2 has a distinctive architecture composed of an N-terminal superfamily I ATPase/helicase domain and a C-terminal

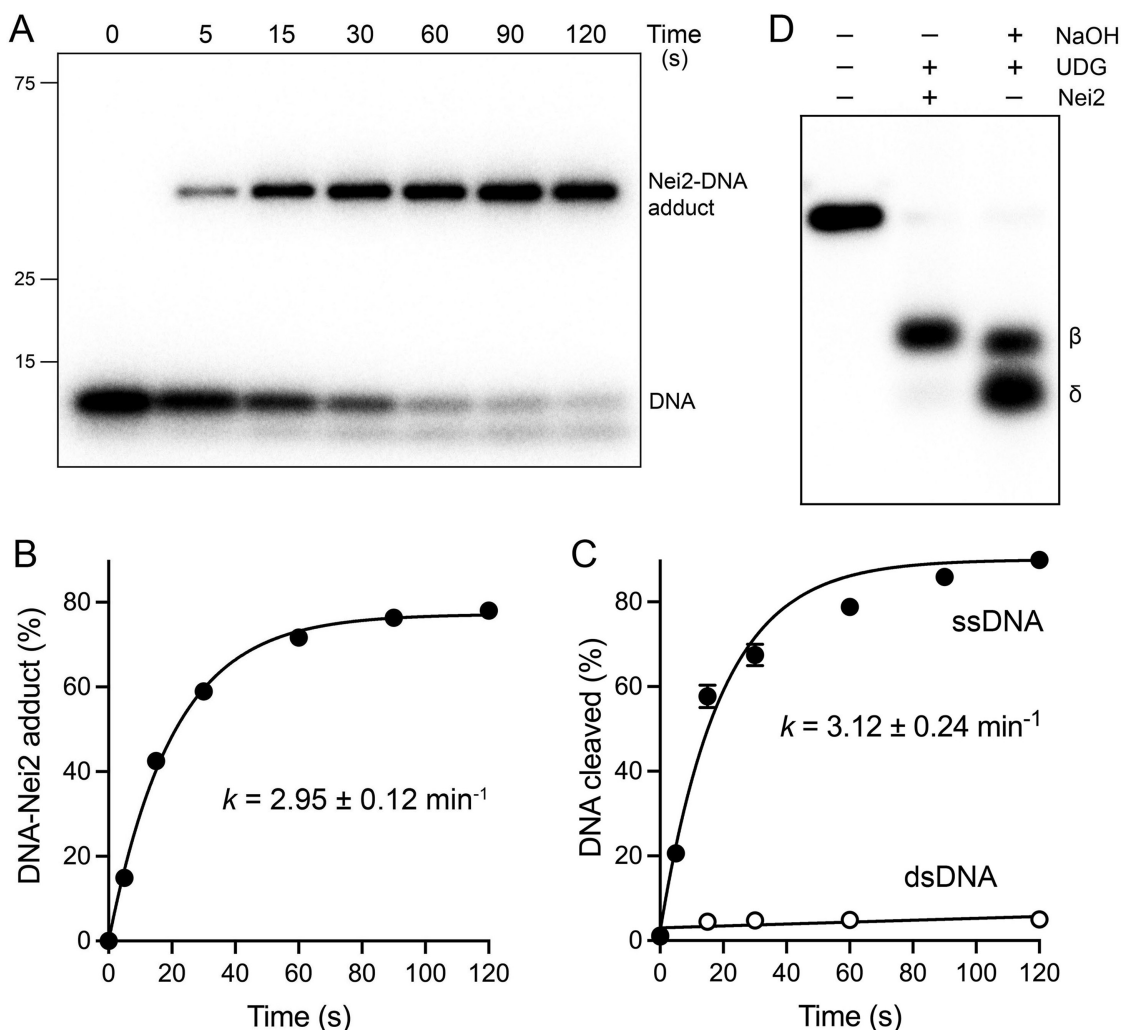


Figure 12. Kinetic analysis of the Nei2 AP lyase reaction. (A) Kinetics of Schiff base formation. A reaction mixture (80 μ l) containing 20 mM Tris-HCl, pH 8.5, 1 mM EDTA, 1 mM DTT, 100 nM (8 pmol) $5'$ 32 P-labeled 24-mer dU-containing DNA oligonucleotide, and 0.64 pmol *E. coli* UDG was pre-incubated at 25°C for 10 min. The reaction mixture was supplemented sequentially with 50 mM NaBH₄ and Nei2 (40 pmol) and then incubated at 25°C. Aliquots (10 μ l) were withdrawn at the times specified and immediately quenched by addition of 2.5 μ l of SDS sample buffer. The products were analyzed by SDS-PAGE in parallel with pre-stained marker polypeptides. 32 P-labeled material was visualized by scanning the gel, which revealed time-dependent formation of a borohydride-trapped covalent Nei2-DNA adduct. (B) The extents of DNA-Nei2 adduct formation (adducted DNA/total DNA in each lane) were calculated in ImageQuant and are plotted as a function of time. Each datum is the average of three independent time course experiments \pm SEM (the error bars fall within the data symbols and are therefore not visible). The data were fit to a one phase association model in Prism, yielding an apparent rate constant for Schiff base formation as shown. (C) Kinetics of abasic DNA cleavage. Reaction mixtures (80 μ l) containing 20 mM Tris-HCl, pH 8.5, 1 mM EDTA, 1 mM DTT, 100 nM (8 pmol) $5'$ 32 P-labeled 24-mer dU-containing DNA oligonucleotide (ssDNA) or 24-bp dU-containing duplex DNA (dsDNA), and 0.64 pmol *E. coli* UDG was pre-incubated at 25°C for 10 min. The UDG pre-treated reaction mixtures were supplemented with Nei2 (40 pmol) and incubated at 25°C. Aliquots (10 μ l) were withdrawn at the times specified and immediately quenched by addition of 10 μ l of a solution containing 90% formamide, 50 mM EDTA, 0.1% bromophenol blue, 0.1% xylene cyanol. The reaction products were analyzed by electrophoresis through a 20% polyacrylamide gel containing 7.5 M urea in 89 mM Tris-borate, 2 mM EDTA. The radiolabeled DNAs were visualized by scanning the gel. The extents of DNA cleavage (incised DNA/total DNA in each lane) were calculated in ImageQuant and are plotted as a function of time. Each datum is the average of three independent time course experiments \pm SEM. The data were fit to a one phase association model in Prism, yielding an apparent rate constant for ssDNA cleavage as shown. (D) The Nei2 AP lyase reaction entails β -elimination. Reaction mixtures (10 μ l) containing 20 mM Tris-HCl, pH 8.5, 1 mM EDTA, 1 mM DTT, 100 nM (1 pmol) $5'$ 32 P-labeled 24-mer dU-containing DNA oligonucleotide, and 0.08 pmol *E. coli* UDG (where indicated by +) were pre-incubated at 25°C for 10 min. One mixture was supplemented with 2 pmol Nei2 (indicated by +) and incubated at 37°C for 10 min. Another mixture was adjusted to 100 mM NaOH (indicated by +) and heated for 5 min at 70°C. After addition of 10 μ l of formamide/EDTA, the products were analyzed by Urea-PAGE and visualized by scanning the gel. Alkaline cleavage of the abasic DNA yields a mixture of β and δ elimination products. Nei2 cleavage is predominantly via β elimination.

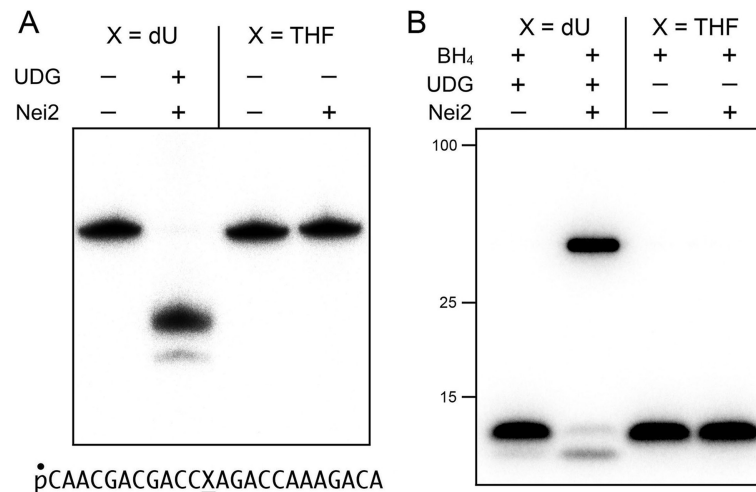


Figure 13. Nei2 is inactive as a lyase at a THF abasic site. Reaction mixtures (20 μl) containing 20 mM Tris-HCl, pH 8.5, 1 mM EDTA, 1 mM DTT, 100 nM (2 pmol) 5' ³²P-labeled 24-mer dU- or THF-containing DNA oligonucleotide (depicted at bottom, where X is dU or THF), and 0.08 pmol *E. coli* UDG (where indicated by +) were pre-incubated at 25°C for 10 min. (A) DNA cleavage. The pre-incubated reaction mixtures were supplemented with 20 pmol Nei2 (where indicated by +) and incubated at 37°C for 30 min. After adding 20 μl of formamide/EDTA, the products were analyzed by Urea-PAGE and visualized by scanning the gel. (B) Schiff base formation. The pre-incubated reaction mixtures were serially adjusted to 50 mM NaBH₄, supplemented with 20 pmol Nei2 (where indicated by +), and then incubated at 37°C for 30 min. The products were analyzed by SDS-PAGE and visualized by scanning the gel. The positions and sizes (kDa) of pre-stained marker polypeptides are indicated on the left.

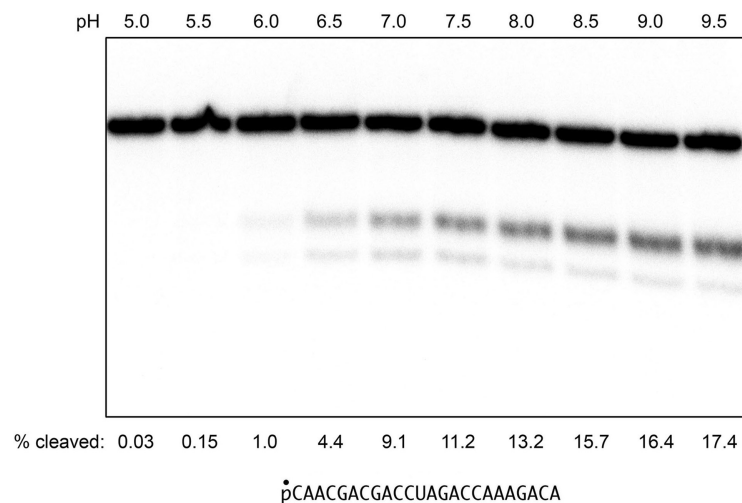


Figure 14. Nei2 is a feeble uracil glycosylase. Reaction mixtures (20 μl) containing 20 mM buffer (either Tris-acetate pH 5.0, 5.5, 6.0 or 6.5 or Tris-HCl pH 7.0, 7.5, 8.0, 8.5, 9.0, or 9.5), 1 mM EDTA, 1 mM DTT, 1 pmol 5' ³²P-labeled 24-mer dU-containing DNA oligonucleotide, and 100 pmol Nei2 were incubated at 25°C for 120 min. After adding 10 μl of formamide/EDTA, the products were analyzed by Urea-PAGE and visualized and quantified by scanning the gel. The extents of DNA cleavage are indicated below the lanes.

HRDC domain, connected by a CxxC-(14-aa)-CxxC tetracysteine module. Whereas the UvrD2 HRDC domain is not required for ATPase or helicase activities *in vitro*, deletion of the tetracysteine module abolishes duplex unwinding while preserving ATP hydrolysis (28). Single alanine mutations in the helicase domain of UvrD2 were identified that either: (i) abolished ATP hydrolysis and helicase activity; or (ii) abolished helicase activity without affecting DNA-dependent ATP hydrolysis (29). When such biochemically defined UvrD2 mutants were deployed to test complementation of ΔuvrD2 lethality in *M. tuberculosis*, it was discovered that neither the HRDC domain nor the tetracysteine module was needed, and that the ATPase activity of UvrD2

was essential for viability but the helicase activity was dispensable (29). In the present study of Lhr, we demonstrate that its repair activities *in vivo* are: (i) contingent on the CTD (i.e. Lhr-Core helicase does not suffice) and its ability to nucleate a homo-tetrameric Lhr quaternary structure; and (ii) dependent on both ATP hydrolysis and duplex unwinding. Mutating the CTD tetramer interface to convert Lhr from a tetramer to a homodimer had no apparent effect on the RNA:DNA helicase activity of full-length Lhr and only a modest effect on DNA:DNA unwinding *in vitro*. This stands in contrast to the complete loss of Lhr DNA repair activity *in vivo* elicited by the interfacial H1199A-R1206A-R1286A mutation.

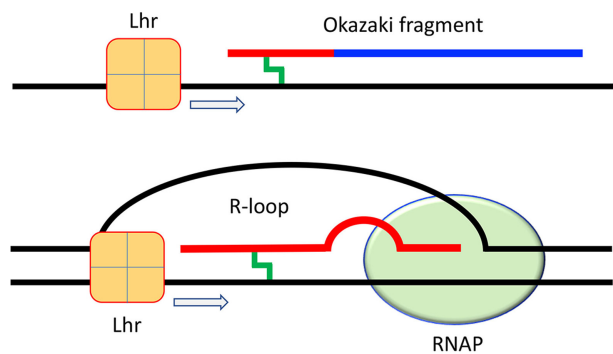


Figure 15. Potential scenarios for Lhr action on RNA:DNA hybrids. (Top panel) Lhr helicase unwinds RNA-primed Okazaki fragments by 3'-to-5' translocation along the DNA tracking strand. The lagging strand DNA template is colored black, the RNA primer is red, and the nascent DNA strand is blue. An RNA:DNA inter-strand crosslink is colored green. (Bottom panel) Lhr unwinds the RNA:DNA hybrid within an R-loop formed when the nascent RNA strand synthesized by RNA polymerase (RNAP) anneals to the template DNA strand. An RNA:DNA inter-strand crosslink is colored green.

An outstanding issue is how, and in what context, the ATPase and helicase activities of Lhr are deployed in crosslink repair. Our thinking on this point is influenced by the finding that Lhr is more active in unwinding an RNA:DNA duplex, via 3'-to-5' translocation on the DNA strand, than it is in unwinding a DNA:DNA duplex (1). This prompts the speculation that Lhr helicase activity might be directed to displacement of the RNA primers of Okazaki fragments (1) or the disengagement of R-loops formed during transcription (Figure 15). Indeed, we envision that Lhr might specialize in repairing RNA–DNA inter-strand crosslinks within Okazaki fragments or R-loops when mycobacteria are treated with MMC or cisplatin. Although only a fraction of the genome would be expected to exist as RNA:DNA hybrid at any given time, the high GC content of the mycobacterial genome provides ample opportunity to form MMC or cisplatin crosslinks to guanine bases in RNA:DNA hybrids. Alternatively, inter-strand DNA:DNA crosslinks might arrest transcribing RNA polymerase and drive formation of R-loops behind the polymerase, upon which Lhr helicase might act, leading to displacement of RNA polymerase from the damaged template so that the damage is accessible to repair machinery.

In conclusion, we propose that Lhr spearheads a distinctive mycobacterial pathway of DNA crosslink repair, possibly abetted by AP lyase and/or glycosylase activities of Nei2. Although a thorough genetic analysis of the impact of deleting Nei2 protein and mutating its active site will be needed to flesh out this scenario, the present characterization of Nei2 brings valuable clarity to what has been, from our perspective, a confounding prior literature. We find that Nei2 is a monomer in solution (not an octamer or dodecamer as suggested earlier). We show that Nei2 is an AP β -lyase enzyme that forms a borohydride-trappable covalent protein-DNA adduct, consistent with the accepted mechanism of Nei/Fpg glycosylase/lyases, which entails formation and resolution of a Schiff base intermediate (22,23). We find that Nei2 does not have lyase activity at a THF abasic site, counter to what had been asserted for GST-

Nei2 (25,26), but consistent with what has been reported for human NEIL1 and mimivirus Nei1 (30). Moreover, we find that Nei2 AP lyase activity displays a strong bias for a single-stranded DNA substrate versus a completely paired duplex DNA, counter to what was published for GST-Nei2 (25), but similar to the single-strand preference characteristic of mammalian NEIL3 (31,32).

Finally, we find that Nei2 displays a feeble uracil glycosylase activity compared to its more vigorous lyase activity, which suggests either of two scenarios regarding Nei2's potential role in crosslink repair: (i) Nei2 functions principally as a lyase that incises AP sites generated by a different glycosylase that excises the crosslinked nucleobase; or (ii) Nei2 has a glycosylase activity that is effective on lesions other than dU, particularly base adducts relevant to crosslinking. Given that Nei2 requires single-stranded DNA character for its lyase activity, it follows that unwinding by a helicase (presumably Lhr) provides a suitable substrate on which Nei2 can act, e.g. a fork structure, as has been shown for crosslink unhooking by NEIL3 (33). An alternative prospect is that Nei2 lyase activity is purposed for avoidance of crosslink formation, specifically the spontaneous occurrence of inter-strand abasic crosslinks in duplex DNA (34), by incising abasic sites (that have been made accessible by helicase unwinding) and thereby preventing reaction of an abasic sugar C1' aldehyde with an adenine amino group on the complementary strand. Our preliminary attempts to demonstrate formation of a binary Lhr-Nei2 complex *in vitro*, by mixing the recombinant proteins and ensuing gel filtration, have not been fruitful, which might suggest either that their interaction entails co-occupancy on a lesion-containing DNA or that their interaction depends on one or more additional mycobacterial protein(s).

DATA AVAILABILITY

The data underlying this article are available in the article and in its online supplementary material.

ACKNOWLEDGEMENTS

This research was supported by NIH grant AI64693 to M.G. and S.S.

FUNDING

U.S. National Institutes of Health [AI64693]. Funding for open access charge: U.S. National Institutes of Health [AI64693].

Conflict of interest statement. M.G. has received consulting fees from Vedanta Biosciences, PRL NYC and Fimbrion Therapeutics and has equity in Vedanta biosciences. Other authors declare no competing interests.

REFERENCES

- Ordenez,H. and Shuman,S. (2013) *Mycobacterium smegmatis* lhr is a DNA-dependent atpase and a 3'-to-5' DNA translocase and helicase that prefers to unwind 3'-tailed RNA:DNA hybrids. *J. Biol. Chem.*, **288**, 14125–14134.
- Ejaz,A., Ordenez,H., Jacewicz,A., Ferrao,R. and Shuman,S. (2018) Structure of mycobacterial 3'-to-5' RNA:DNA helicase lhr bound to

- a ssDNA tracking strand highlights distinctive features of a novel family of bacterial helicases. *Nucleic Acids Res.*, **46**, 442–455.
3. Warren, G.M., Wang, J., Patel, D.J. and Shuman, S. (2021) Oligomeric quaternary structure of *Escherichia coli* and *Mycobacterium smegmatis* Ihr helicases is nucleated by a novel C-terminal domain composed of five winged-helix modules. *Nucleic Acids Res.*, **49**, 3876–3887.
 4. Wang, S., Liu, K., Xiao, L., Yang, L., Li, H., Zhang, F., Lei, L., Li, S., Feng, X., Li, A. *et al.* (2016) Characterization of a novel DNA glycosylase from *S. sahachiroi* involved in the reduction and repair of azinomycin B induced DNA damage. *Nucleic Acids Res.*, **44**, 187–197.
 5. Mullins, E.A., Warren, G.M., Bradley, N.P. and Eichman, B.F. (2017) Structure of a DNA glycosylase that unhooks interstrand cross-links. *Proc. Natl. Acad. Sci. U.S.A.*, **114**, 4400–4405.
 6. Rand, L., Hinds, J., Springer, B., Sander, P., Buxton, R.S. and Davis, E.O. (2003) The majority of inducible DNA repair genes in *Mycobacterium tuberculosis* are induced independently of RecA. *Mol. Microbiol.*, **50**, 1031–1042.
 7. Boshoff, H.I.M., Reed, M.B., Barry, C.E. and Mizrahi, V. (2003) DnaE2 polymerase contributes to in vivo survival and the emergence of drug resistance in *Mycobacterium tuberculosis*. *Cell*, **113**, 183–193.
 8. Müller, A.U., Imkamp, F. and Weber-Ban, E. (2018) The mycobacterial LexA/RecA-Independent DNA damage response is controlled by PafBC and the pup-Proteasome system. *Cell Rep.*, **23**, 3551–3564.
 9. Brzostek, A., Plocinski, P., Minias, A., Ciszewska, A., Gasior, F., Pawelczyk, J., Dziadek, B., Slomka, M. and Dziadek, J. (2021) Dissecting the RecA-(In)dependent response to mitomycin C in *Mycobacterium tuberculosis* using transcriptional profiling and proteomics analyses. *Cells*, **10**, 1168.
 10. Adefisayo, O.O., Dupuy, P., Nautiyal, A., Bean, J.M. and Glickman, M.S. (2021) Division of labor between SOS and PafBC in mycobacterial DNA repair and mutagenesis. *Nucleic Acids Res.*, **49**, 12805–12819.
 11. Chengalroyen, M.D., Mason, M.K., Borsellini, A., Tassoni, R., Abrahams, G.L., Lynch, S., Ahn, Y.M., Ambler, J., Young, K., Crowley, B.M. *et al.* (2022) DNA-dependent binding of nargenicin to DnaE1 inhibits replication in *Mycobacterium tuberculosis*. *ACS Infect. Dis.*, **8**, 612–625.
 12. DeJesus, M.A., Gerrick, E.R., Xu, W., Park, S.W., Long, J.E., Boutte, C.C., Rubin, E.J., Schnappinger, D., Ehrt, S., Fortune, S.M. *et al.* (2017) Comprehensive essentiality analysis of the *Mycobacterium tuberculosis* genome via saturating transposon mutagenesis. *Mbio*, **8**, e02133-16.
 13. Bosch, B., DeJesus, M.A., Poulton, N.C., Zhang, W., Engelhart, C.A., Zaveri, A., Lavalette, S., Ruecker, N., Trujillo, C., Wallach, J.B. *et al.* (2021) Genome-wide gene expression tuning reveals diverse vulnerabilities of *M. tuberculosis*. *Cell*, **184**, 4579–4592.
 14. Barkan, D., Stallings, C.L. and Glickman, M.S. (2011) An improved counterselectable marker system for mycobacterial recombination using *galK* and 2-deoxy-galactose. *Gene*, **470**, 31–36.
 15. Sinha, K.M., Stephanou, N.C., Gao, F., Glickman, M.S. and Shuman, S. (2007) Mycobacterial UvrD1 is a Ku-dependent DNA helicase that plays a role in multiple DNA repair events, including double-strand break repair. *J. Biol. Chem.*, **282**, 15114–15125.
 16. Paz, M.M., Ladwa, S., Champeil, E., Liu, Y., Rockwell, S., Boamah, E.K., Bargonetti, J., Callahan, J., Roach, J. and Tomasz, M. (2008) Mapping DNA adducts of mitomycin C and decarbamoyl mitomycin C in cell lines using liquid chromatography/electrospray tandem mass spectrometry. *Chem. Res. Toxicol.*, **21**, 2370–2378.
 17. Ghosh, S. (2019) Cisplatin: the first metal based anticancer drug. *Bioorg. Chem.*, **88**, 102925.
 18. Mullins, E.A., Rodriguez, A.A., Bradley, N.P. and Eichman, B.F. (2019) Emerging roles of DNA glycosylases and the base excision repair pathway. *TIBS*, **44**, 765–781.
 19. Semlow, D.R., Zhang, J., Budzowska, M., Drohat, A.C. and Walter, J.C. (2016) Replication-dependent unhooking of DNA interstrand cross-links by the NEIL3 glycosylase. *Cell*, **167**, 498–511.
 20. Nejad, M.I., Housh, K., Rodriguez, A.A., Haldar, T., Kathe, S., Wallace, S.S., Eichman, B.F. and Gates, K.S. (2020) Unhooking of an interstrand cross-link at DNA fork structures by the DNA glycosylase NEIL3. *DNA Repair*, **86**, 102752.
 21. Li, N., Wang, J., Wallace, S.S., Chen, J., Zhou, J. and D'Andrea, A.D. (2020) Cooperation of the NEIL3 and Fanconi anemia/BRCA pathways in interstrand crosslink repair. *Nucleic Acid Res.*, **48**, 3014–3028.
 22. Zharkov, D.O., Golan, G., Gilboa, R., Fernandes, A.S., Gerchman, S.E., Kycia, J.H., Rieger, R.A., Grollman, A.P. and Shoham, G. (2002) Structural analysis of an *Escherichia coli* endonuclease VIII covalent reaction intermediate. *EMBO J.*, **21**, 789–800.
 23. Gilboa, R., Zharkov, D.O., Golan, G., Fernandes, A.S., Gerchman, S.E., Matz, E., Kycia, J.H., Grollman, A.P. and Shoham, G. (2002) Structure of formamidopyrimidine-DNA glycosylase covalently complexed to DNA. *J. Biol. Chem.*, **277**, 19811–19816.
 24. Guo, Y., Bandaru, V., Jaruga, P., Zhao, X., Burrows, C.J., Iwai, S., Dizdaroğlu, M., Bond, J.P. and Wallace, S.S. (2010) The oxidative DNA glycosylases of *mycobacterium tuberculosis* exhibit different substrate preferences from their *Escherichia coli* counterparts. *DNA Repair*, **9**, 177–190.
 25. Lata, K., Afsar, M. and Ramachandran, R. (2017) Biochemical characterization and novel inhibitor identification of *Mycobacterium tuberculosis* endonuclease VIII 2 (Rv3297). *Biochem. Biophys. Rep.*, **12**, 20–28.
 26. Lata, K., Vishwakarma, J., Kumar, S., Khanam, T. and Ramachandran, R. (2022) *Mycobacterium tuberculosis* endonuclease VIII 2 (Nei2) forms a prereplicative BER complex with DnaN: identification, characterization, and disruption of complex formation. *Mol. Microbiol.*, **117**, 320–333.
 27. Güthlein, C., Wanner, R.M., Sander, P., Davis, E.O., Bosshard, M., Jiricny, J., Böttger, E.C. and Springer, B. (2009) Characterization of the mycobacterial NER system reveals novel functions of the *uvrDI* helicase. *J. Bacteriol.*, **191**, 555–562.
 28. Sinha, K.M., Stephanou, N.C., Unciuleac, M.C., Glickman, M.S. and Shuman, S. (2008) Domain requirements for DNA unwinding by mycobacterial UvrD2, an essential DNA helicase. *Biochemistry*, **47**, 9355–9364.
 29. Williams, A., Güthlein, C., Beresford, N., Böttger, E.C., Springer, B. and Davis, E.O. (2011) UvrD2 is essential in *mycobacterium tuberculosis*, but its helicase activity is not required. *J. Bacteriol.*, **193**, 4487–4494.
 30. Imamura, K., Wallace, S.S. and Doublé, S. (2009) Structural characterization of a viral NEIL1 ortholog unliganded and bound to abasic site-containing DNA. *J. Biol. Chem.*, **284**, 26174–26183.
 31. Liu, M., Bandaru, V., Bond, J.P., Jaruga, P., Zhao, X., Christov, P.P., Burrows, C.J., Rizzo, C.J., Dizdaroğlu, M. and Wallace, S.S. (2010) The mouse ortholog of NEIL3 is a functional DNA glycosylase in vitro and in vivo. *Proc. Natl. Acad. Sci. U.S.A.*, **107**, 4925–4930.
 32. Liu, M., Imamura, K., Averill, A.M., Wallace, S.S. and Doublé, S. (2013) Structural characterization of a mouse ortholog of human NEIL3 with a marked preference for single-stranded DNA. *Structure*, **21**, 247–256.
 33. Nejad, M.I., Housh, K., Rodriguez, A.A., Haldar, T., Kathe, S., Wallace, S.S., Eichman, B.F. and Gates, K.S. (2020) Unhooking of an interstrand cross-link at DNA fork structures by the DNA glycosylase NEIL3. *DNA Repair*, **86**, 102752.
 34. Huskova, A., Landova, B., Boura, E. and Silhan, J. (2022) The rate of formation and stability of abasic site interstrand crosslinks in the DNA duplex. *DNA Repair*, **113**, 103300.